Ubc13–Mms2 cooperates with a family of RING E3 proteins in budding yeast membrane protein sorting

Christian Renz, Véronique Albanèse, Vera Tröster, Thomas Albert, Olivier Santt, Susan Jacobs, Anton Khmelinskii, Sébastien Léon, Helle Ulrich

© 2020. Published by The Company of Biologists Ltd | Journal of Cell Science (2020) 133, jcs244566. doi:10.1242/jcs.244566

RESEARCH ARTICLE

Ubc13–Mms2 cooperates with a family of RING E3 proteins in budding yeast membrane protein sorting

Christian Renz[1], Véronique Albanèse[2], Vera Tröster[1], Thomas K. Albert[3,*], Olivier Santt[4,‡], Susan C. Jacobs[4,§], Anton Khmelinskii[1], Sébastien Léon[2] and Helle D. Ulrich[1,¶]

ABSTRACT

Polyubiquitin chains linked via lysine (K) 63 play an important role in endocytosis and membrane trafficking. Their primary source is the ubiquitin protein ligase (E3) Rsp5/NEDD4, which acts as a key regulator of membrane protein sorting. The heterodimeric ubiquitin-conjugating enzyme (E2), Ubc13–Mms2, catalyses K63-specific polyubiquitylation in genome maintenance and inflammatory signalling. In budding yeast, the only E3 proteins known to cooperate with Ubc13–Mms2 so far is a nuclear RING finger protein, Rad5, involved in the replication of damaged DNA. Here, we report a contribution of Ubc13–Mms2 to the sorting of membrane proteins to the yeast vacuole via the multivesicular body (MVB) pathway. In this context, Ubc13–Mms2 cooperates with Pib1, a FYVE-RING finger protein associated with internal membranes. Moreover, we identified a family of membrane-associated FYVE-(type)-RING finger proteins as cognate E3 proteins for Ubc13–Mms2 in several species, and genetic analysis indicates that the contribution of Ubc13–Mms2 to membrane trafficking in budding yeast goes beyond its cooperation with Pib1. Thus, our results widely implicate Ubc13–Mms2 as an Rsp5-independent source of K63-linked polyubiquitin chains in the regulation of membrane protein sorting.

This article has an associated First Person interview with the first author of the paper.

KEY WORDS: FYVE domain, K63-polyubiquitylation, Membrane protein sorting, RING finger, Ubiquitin protein ligase, Ubiquitin-conjugating enzyme

INTRODUCTION

Post-translational modification with ubiquitin serves as a versatile means to modulate protein function, not least because of the diversity of ubiquitin signals (Kwon and Ciechanover, 2017). Ubiquitin is usually attached to its substrates via an isopeptide bond between its C-terminus and an internal lysine (K) residue of the target protein. Modification is accomplished by the successive action of a ubiquitin-activating enzyme (E1), a ubiquitin-conjugating enzyme (E2) and a ubiquitin protein ligase (E3). Ubiquitin itself can serve as a target for further modification. Depending on which of its seven lysine residues is used as an acceptor for conjugation, polyubiquitin chains are formed with varying topology (Komander and Rape, 2012). Downstream effector proteins that recognise the modification via dedicated ubiquitin-binding domains mediate the biological effects (Husnjak and Dikic, 2012). As a consequence, ubiquitylation can impinge on the conformation, localisation or interactions of the modified protein. Polyubiquitin chain linkage is thought to play an important role in specifying the consequences of ubiquitylation. Whereas K48-, K11- and K29-linked polyubiquitylation have been implicated in proteasomal degradation, the K63-linkage is involved in the regulation of numerous non-proteasomal pathways ranging from the DNA damage response to inflammatory signalling, endocytosis, intracellular membrane trafficking and lysosomal targeting (Erpapazoglou et al., 2014; García-Rodríguez et al., 2016; Panier and Durocher, 2009; Wu and Karin, 2015).

The topology of a polyubiquitin chain is determined by the enzymes involved in its assembly (Suryadinata et al., 2014). Among the characterised E2s, Ubc13 is unique in exclusively generating K63-linked chains. Its linkage specificity arises from an obligatory interaction partner, the catalytically inactive E2 variant Mms2 (Hofmann and Pickart, 1999). Ubc13 cooperates with a number of E3s, such as human TRAF6, CHFR, RNF8, RNF168 and CHIP (Hodge et al., 2016). In the budding yeast, *Saccharomyces cerevisiae*, the only E3 known to function with Ubc13 is Rad5, which is involved in DNA damage bypass (Ulrich and Jentsch, 2000). All these E3s belong to the RING finger or the related U-box families and, in each case, Ubc13 apparently dictates linkage specificity (Zheng and Shabek, 2017). When combined with other E2s, some RING E3s, such as CHIP, can assemble polyubiquitin chains of alternative or even mixed linkages (Kim et al., 2007). In contrast to the RING and U-box proteins, E3s of the HECT and RBR families directly determine chain linkage. For example, the budding yeast HECT E3 Rsp5 predominantly catalyses ubiquitin polymerisation via K63 (Erpapazoglou et al., 2014). Most probably, the influence of these E3 families on linkage selectivity is due to their direct participation in the thioester-mediated transfer of ubiquitin to the acceptor lysine.

Together, Rsp5 (or its mammalian homologue NEDD4) and Ubc13 appear to be responsible for the bulk of K63-polyubiquitylation in yeast and vertebrate cells. Rsp5/NEDD4 is mainly involved in membrane trafficking, mediating ubiquitylation of various plasma membrane proteins and components of the endocytic machinery (Erpapazoglou et al., 2014). Human UBC13 (also called UBE2N) cooperates with the E2 variant UBE2V2 (also called MMS2) in genome maintenance-related functions in the

[1]Institute of Molecular Biology gGmbH (IMB), Ackermannweg 4, D-55128 Mainz, Germany. [2]Institut Jacques Monod, UMR 7592 Centre National de la Recherche Scientifique/Université Paris-Diderot, Sorbonne Paris Cité, 75205 Paris Cedex 13, France. [3]Max Planck Institute for Terrestrial Microbiology, Karl-von-Frisch-Str. 10, D-35043 Marburg, Germany. [4]Cancer Research UK London Research Institute, Clare Hall Laboratories, Blanche Lane, South Mimms EN6 3LD, UK.
*Present address: University Children's Hospital Muenster, Department of Pediatric Hematology and Oncology, D-48149 Muenster, Germany. ‡Present address: Centre de Recherche en Biologie cellulaire de Montpellier, UMR 5237 Centre National de la Recherche Scientifique, 1919 route de Mende, 34293 Montpellier Cedex 05, France. §Present address: The Pirbright Institute, Ash Road, Woking GU24 0NF, United Kingdom.

¶Author for correspondence (h.ulrich@imb-mainz.de)

V.A., 0000-0002-5947-7415; O.S., 0000-0002-7896-7209; S.C.J., 0000-0001-5499-6323; A.K., 0000-0002-0256-5190; S.L., 0000-0002-2536-8595; H.D.U., 0000-0003-0431-2223

Handling Editor: Tamotsu Yoshimori
Received 25 January 2020; Accepted 23 March 2020

Journal of Cell Science

Journal of Cell Science (2020) 133, jcs244566. doi:10.1242/jcs.244566

nucleus, while in the cytoplasm it associates with UBE2V1 (also called UEV1A) for inflammatory signalling in the NF-κB pathway (Andersen et al., 2005). Surprisingly, in budding yeast, which lacks an NF-κB pathway, Ubc13–Mms2 also localises mainly to the cytoplasm and accumulates in the nucleus only in response to DNA damage (Ulrich and Jentsch, 2000), thus raising the question of its cytoplasmic function.

Here, we report that Ubc13–Mms2 from *S. cerevisiae* can act as a cognate E2 for a family of RING E3s associated with membranes of the endocytic and lysosomal compartments. Our findings are based on the identification of a poorly characterised RING E3, Pib1, as an interactor of Ubc13 and Mms2 in a two-hybrid screen. Pib1 localises to endosomal and vacuolar membranes via a lipid-binding FYVE domain (Burd and Emr, 1998; Shin et al., 2001) and plays a role in the multivesicular body (MVB) pathway where it acts redundantly with an Rsp5 adaptor, Bsd2, in delivering plasma membrane proteins to the vacuole (Nikko and Pelham, 2009). We found that Pib1 is highly selective for Ubc13–Mms2 in terms of both physical interaction and activation of ubiquitin transfer, and that the proteins cooperate *in vivo* as a K63-specific E2–E3 pair. Moreover, we observed a comparable activity with Ubc13–Mms2 in a series of other RING finger proteins associated with membranes of the endocytic and lysosomal compartments. Some of these share the FYVE-RING domain arrangement of Pib1, such as the postulated Pib1 homologue from *Schizosaccharomyces pombe* (SpPib1, also known as Putative E3 ubiquitin-protein ligase C36B7.05c) (Kampmeyer et al., 2017), a protein from *Ustilago maydis* involved in mRNP particle transport (Upa1, also known as UMAG_12183) (Pohlmann et al., 2015) and human Rififylin (RFFL, also known as CARP2 or Sakura), which harbours a FYVE-like domain (Coumailleau et al., 2004). Consistent with these interactions, Ubc13–Mms2 functionally contributes to the delivery of membrane proteins to the vacuole via the MVB pathway, where it cooperates with Pib1, but also exhibits additional Pib1-independent activity. In combination with an analysis of genetic interactions, our data widely implicate Ubc13–Mms2 as a significant Rsp5-independent source of K63-polyubiquitin chains in the regulation of intracellular membrane protein sorting and turnover.

RESULTS

Ubc13 interacts with the dimeric RING finger protein Pib1

In an effort to identify potential regulators of the heterodimeric E2 complex Ubc13–Mms2, we performed a two-hybrid screen using the *S. cerevisiae* E2 variant Mms2 as a bait. From a budding yeast genomic library of ∼5×10^6 clones (James et al., 1996), we obtained at least five independent isolates encoding the full sequence of Pib1 as the only verifiable interactor. This 286 amino acid protein harbours an N-terminal FYVE domain and a C-terminal RING finger (Fig. 1A) (Burd and Emr, 1998). When analysed individually in two-hybrid assays, Pib1 exhibited a moderate interaction with Mms2 in only one of the two orientations of the system, but interacted more strongly with Ubc13 (Fig. 1B). Mutation of conserved Pib1 residues critical for E2 interaction in other RING finger proteins (C225A or I227A) (Metzger et al., 2014) abolished association with both Ubc13 and Mms2 (Fig. S1A), suggesting an involvement of the RING finger in E2 binding.

The robust interaction between Pib1 and Ubc13 pointed to a direct association, whereas the weak interaction between Pib1 and Mms2 might reflect an indirect contact mediated by endogenous Ubc13 in the two-hybrid assay. We therefore deleted either *UBC13* or *MMS2* in the reporter strain (Fig. 1C). Consistent with an Ubc13-mediated indirect interaction between Pib1 and Mms2, the two-hybrid signal was abolished in the *ubc13Δ* background. Surprisingly, deletion of *MMS2* also weakened the interaction between Pib1 and Ubc13 in one orientation, suggesting a contribution of Mms2 to the interaction between Pib1 and the E2. Mutations in Ubc13 corresponding to positions that generally mediate RING binding in E2s, such as K6, K10, M64 and S96, also

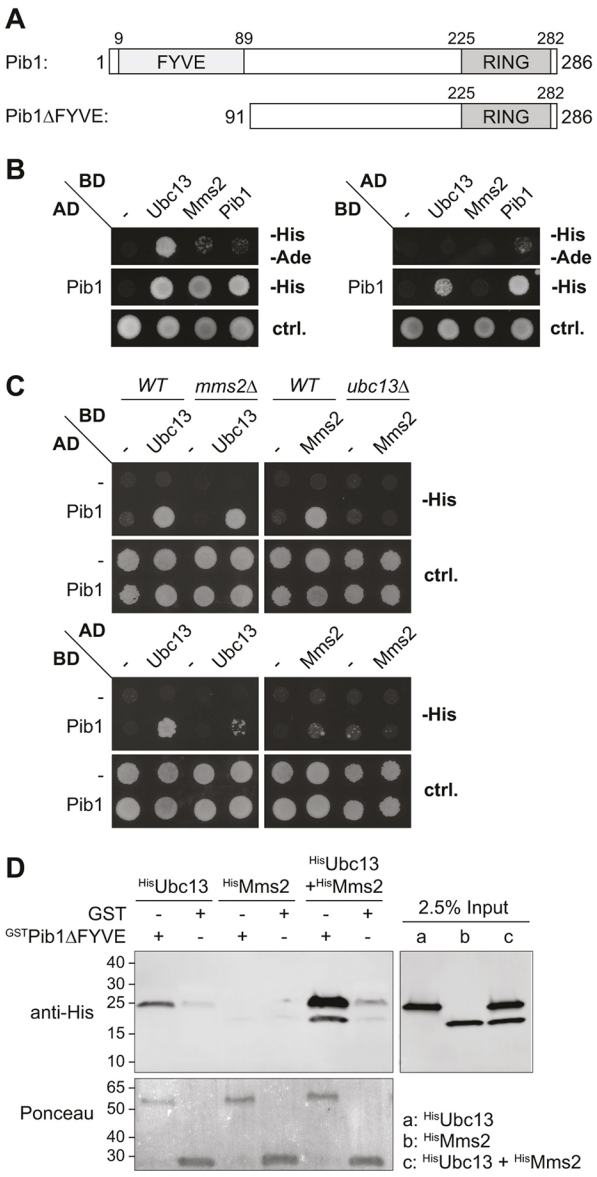

Fig. 1. Pib1 interacts with Ubc13 in a manner that is enhanced by Mms2. (A) Schematic representation of Pib1 domain structure. (B) Interactions of Pib1 with Ubc13, Mms2 and itself in the two-hybrid assay (AD, Gal4 activation domain; BD, Gal4 DNA-binding domain). Growth on -His medium indicates positive interactions; growth on -His-Ade medium indicates strong associations. Growth on control medium containing His and Ade is also shown (ctrl.). Images shown are representative of $n>3$ experiments. (C) Pib1–Mms2 interaction is mediated by Ubc13. Two-hybrid analysis was performed as in B using *mms2Δ* or *ubc13Δ* mutant reporter strains. Images shown are representative of $n=2$ experiments. (D) Mms2 requires Ubc13 for interaction with Pib1 *in vitro*. Association of recombinant ^{GST}Pib1ΔFYVE with ^{His}Ubc13 and ^{His}Mms2 was assessed by pre-loading ^{GST}Pib1ΔFYVE or GST onto glutathione Sepharose before incubation with 1 µM recombinant ^{His}Ubc13, ^{His}Mms2 or ^{His}Ubc13–^{His}Mms2 complex. Bound material was detected by western blotting with an anti-His_6-tag antibody and Ponceau staining of the membrane. Blots shown are representative of $n=4$ experiments.

Journal of Cell Science (2020) 133, jcs244566. doi:10.1242/jcs.244566

affected the Pib1–Ubc13 interaction (Fig. S1B). This indicates that Ubc13 contacts the Pib1 RING domain in a 'standard' orientation that is comparable to its interaction with other E3s, including Rad5 (Metzger et al., 2014; Ulrich, 2003).

We confirmed the direct interaction of Pib1 with Ubc13–Mms2 *in vitro* by immobilising recombinant, GST-tagged Pib1ΔFYVE on glutathione Sepharose and examining retention of the E2. Consistent with the two-hybrid data, Ubc13 alone or in complex with Mms2 bound to ^{GST}Pib1ΔFYVE, whereas Mms2 failed to interact with ^{GST}Pib1ΔFYVE in the absence of Ubc13 (Fig. 1D). Again, the presence of Mms2 enhanced the interaction between Ubc13 and Pib1.

In the two-hybrid assay, association of Pib1 with itself was also noted (Fig. 1B). Size-exclusion chromatography analysis of a series of recombinant Pib1 truncation constructs revealed a running behaviour consistent with dimerisation, mediated by a sequence N-terminal to, and including, the RING finger. The minimal region adjacent to the RING domain required for robust dimerisation was found to be between 50 and 100 amino acids in length (Fig. S1C).

Pib1 is an E3 with high selectivity for Ubc13–Mms2

Our results suggested that Pib1 acts as a cognate E3 for Ubc13–Mms2. Indeed, *in vitro* ubiquitin polymerisation by Ubc13–Mms2 was strongly stimulated by the addition of Pib1ΔFYVE in a concentration-dependent manner (Fig. 2A). Chain formation proceeded exclusively via K63, as mutant ubiquitin, Ub(K63R), was not polymerised at all (Fig. 2B), and the K63-specific ubiquitin isopeptidase AMSH (McCullough et al., 2004) efficiently disassembled the products of the Pib1-stimulated reaction (Fig. 2C). Comparison of the *in vitro* activities of Pib1 truncation constructs showed a correlation between stimulation of polyubiquitin chain synthesis and Pib1 dimerisation, indicating that Pib1 is more effective as a dimer than as a monomer, but its FYVE domain is not required for catalytic activity (Fig. S2A).

As some E3s can function with multiple E2s, we asked how specific the Pib1–Ubc13–Mms2 interaction was. In fact, Pib1 has previously been reported to cooperate with one of the most non-selective human E2s, UBCH5A (also known as UBE2D1), *in vitro* (Shin et al., 2001); however, these observations were made using GST-tagged versions of both Pib1 and the E2, which might have induced inappropriate E2–E3 pairing. In a systematic two-hybrid assay with all budding yeast E2s, Pib1 exclusively interacted with Ubc13 and Mms2 (Fig. S2B–D). *In vitro* interaction assays with ^{GST}Pib1ΔFYVE showed no significant binding to a range of recombinant yeast E2s, including Rad6, Cdc34, Ubc7 and two highly promiscuous UBCH5A homologues, Ubc4 and Ubc5 (Fig. 2D). Moreover, and consistent with a high selectivity for Ubc13–Mms2, Pib1ΔFYVE did not stimulate ubiquitin polymerisation by Ubc4 or Ubc7 (Fig. 2E), even though both E2s were active in combination with appropriate partners, Rsp5 and Cue1 (Bazirgan and Hampton, 2008), respectively (Fig. 2F,G). Notably, Rsp5 and Cue1 activated only their cognate E2, but not Ubc13–Mms2, thus indicating selectivity on the side of the E2s as well.

In order to exclude the possibility that the failure of Pib1 to activate Ubc4 was due to the lack of a suitable substrate, we performed thioester discharge assays with Ubc13 and Ubc4. Here, the ability of an E3 to stimulate E2 activity is measured by its effect on a substrate-independent discharge of the ubiquitin thioester from the E2 to free lysine (Branigan et al., 2015). In order to prevent an intramolecular attack on the catalytic cysteine in Ubc13 or Ubc4, we used E2 mutants, Ubc13(K92R) and Ubc4(K91R), which are catalytically active but resistant to autoubiquitylation (McKenna et al., 2001). Consistent with its high selectivity for Ubc13, Pib1 promoted the discharge of the Ubc13 thioester (Ubc13~Ub), but not the Ubc4 thioester (Ubc4~Ub), whereas effective discharge of Ubc4~Ub was observed with Rsp5 (Fig. 2H,I).

Based on these observations, we conclude that Pib1 acts as an E3 with high selectivity for Ubc13–Mms2, and – as was observed with other RING E3s – the E2 dictates the linkage specificity of the reaction.

Ubc13–Mms2 cooperates with multiple RING E3s associated with internal membranes

Pib1 shares its domain arrangement with a number of proteins from other organisms (Fig. 3A). The FYVE domain in association with a RING finger is conserved among fungi such as *S. pombe* and *U. maydis*, whereas FYVE-like domains lacking the characteristic WxxD signature motif can be found in metazoan RING finger proteins such as human RFFL (Stenmark and Aasland, 1999; Tibbetts et al., 2004). We thus asked whether the selectivity for Ubc13–Mms2-mediated K63-polyubiquitylation would extend to other members of this FYVE-(type)-RING protein family: *S. pombe* SpPib1, *U. maydis* Upa1 and human RFFL. We also analysed two additional RING E3s associated with the endocytic compartment: the integral membrane protein Tul1 from *S. cerevisiae*, which localises to endosomal, Golgi and vacuolar membranes (Li et al., 2015; Reggiori and Pelham, 2002), and human ZNRF2, which lacks a FYVE domain, but is targeted to internal membranes via myristoylation and was reported to be an orthologue of SpPib1 (Araki and Milbrandt, 2003; Wood et al., 2012). Finally, we included an ER-associated budding yeast RING E3, Hrd1, as a representative of a distinct subcellular compartment (Bays et al., 2001).

Systematic two-hybrid assays (Fig. 3B and Fig. S3) revealed interactions of the fungal FYVE-RING proteins with budding yeast Ubc13 and with its human homologue (UBC13, also known as UBE2N) and weaker interactions with the Ubc13 cofactors, Mms2 and the human E2 variants, UBE2V1 and UBE2V2. In addition, SpPib1 displayed robust interactions with a range of human E2s, among them members of the UBCH5 family (UBE2D1, UBE2D2 and UBE2D3). A similar, possibly even less selective interaction pattern was observed for ZNRF2. In contrast, RFFL did not show any strong interactions in the two-hybrid assay. The cytoplasmic domain of Tul1 displayed weak interaction with Ubc13, but also with Ubc6 and a number of human E2s, including the UBCH5 family and UBE2V1. A C-terminal construct of Hrd1 did not exhibit measurable interactions with any yeast E2s, but with some human E2s, including UBC13 (UBE2N).

Stable associations between E2 and RING finger proteins do not necessarily correlate with efficient cooperation in ubiquitin transfer (Lorick et al., 1999). Therefore, we performed *in vitro* ubiquitin polymerisation assays using the purified E3s in combination with budding yeast Ubc4, Ubc7 and Ubc13–Mms2. All of the RING finger proteins strongly stimulated Ubc13–Mms2 in K63-polyubiquitylation (Fig. 3C–H), indicating that robust interactions are not required for productive cooperation. In contrast, only Hrd1 stimulated Ubc7 activity but only in the presence of Cue1 (Fig. 3H and Fig. S4A). Hrd1 and RFFL also promoted the assembly of ubiquitin conjugates by Ubc4. For the latter E2–E3 pair, use of a series of ubiquitin mutants indicated a diverse set of linkages and attachment sites among the conjugates, as only a lysine-less ubiquitin variant significantly interfered with their assembly (Fig. S4B).

In order to exclude the possibility that the observed selectivities were due to species-specific features, we repeated the ubiquitin polymerisation assays with the recombinant human E2s, UBC13–UBE2V2 and UBCH5A. As expected, human

Journal of Cell Science (2020) 133, jcs244566. doi:10.1242/jcs.244566

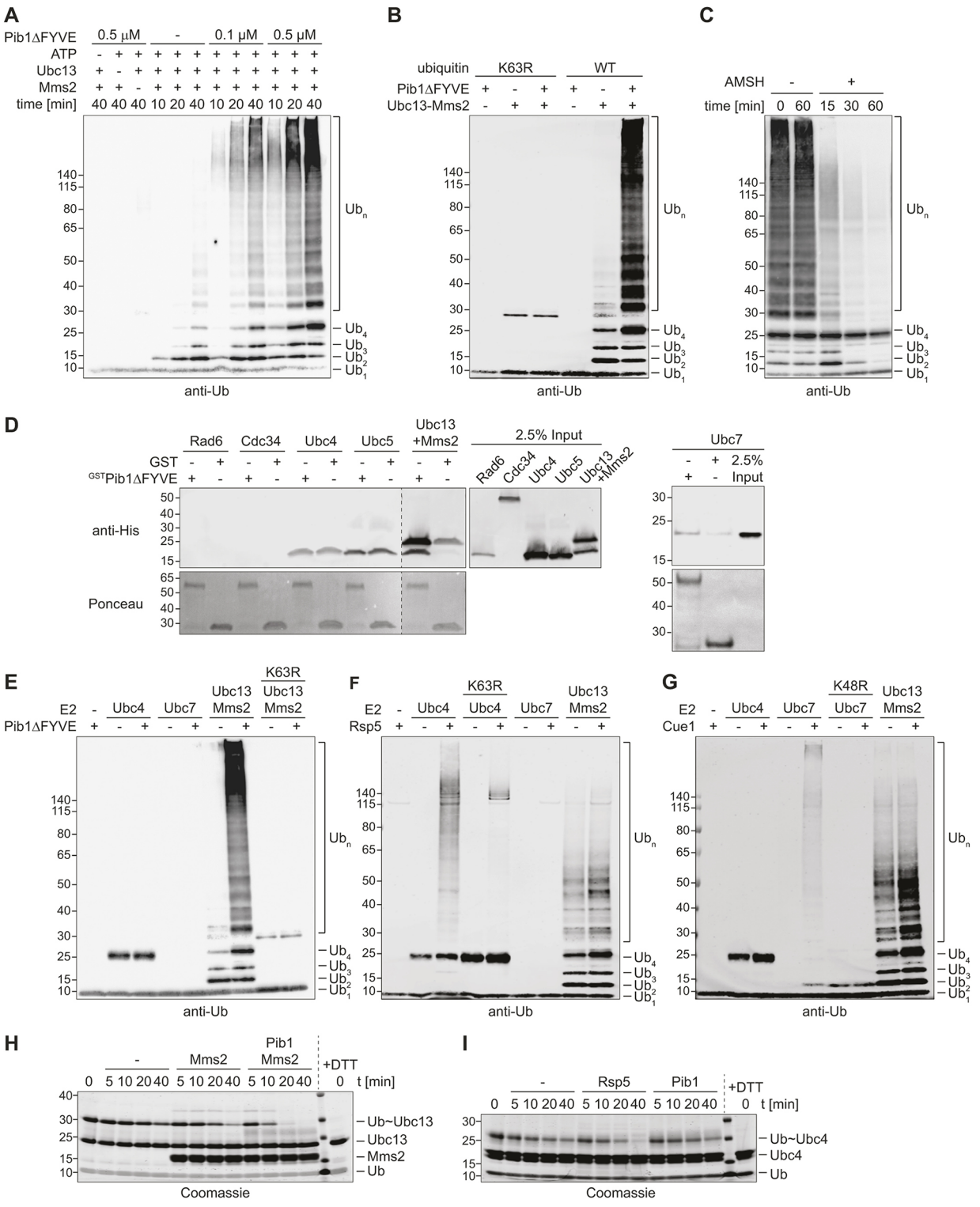

Fig. 2. See next page for legend.

UBC13–UBE2V2 was active with both human E3s (Fig. S4C). Human UBCH5A proved even less selective than its yeast homologue, Ubc4, cooperating at least to some degree with all the constructs tested (Fig. S4C). However, stimulation of Pib1 by UBCH5A was marginal compared to Ubc13–Mms2 or UBC13–UBE2V2.

Taken together, these observations suggest that K63-specific polyubiquitylation in cooperation with Ubc13–Mms2 may be a salient feature of an entire group of membrane-associated RING E3s. Although some of them also appear to be able to cooperate with other E2s, possibly resulting in alternative linkages, Pib1 is one of the most highly selective E3s.

Journal of Cell Science (2020) 133, jcs244566. doi:10.1242/jcs.244566

Fig. 2. Pib1 is an E3 with high selectivity for Ubc13–Mms2. (A) Pib1 stimulates *in vitro* polyubiquitin chain synthesis by Ubc13–Mms2. Recombinant ^{GST}Pib1ΔFYVE, ^{His}Ubc13 and untagged Mms2, as well as ATP, were added as indicated to reactions containing E1 and ubiquitin and incubated at 30°C for the indicated times. Products were analysed by western blotting with an anti-ubiquitin antibody. (B) Pib1 selectively stimulates the synthesis of K63-linked polyubiquitin chains. *In vitro* ubiquitylation reactions were set up as in A, using WT or a K63R mutant ubiquitin, and incubated at 30°C for 30 min. (C) Pib1-catalysed chains are disassembled by the K63-specific ubiquitin isopeptidase AMSH. Conjugation reactions like those shown in B were terminated by addition of apyrase, followed by further incubation in the presence or absence of ^{GST}AMSH at 37°C for the indicated times. (D) Pib1 selectively interacts with Ubc13–Mms2. Interaction of ^{GST}Pib1ΔFYVE with ^{His}Rad6, ^{His}Cdc34, ^{His}Ubc4, ^{His}Ubc5, ^{His}Ubc13-^{His}Mms2 and ^{His}Ubc7 was analysed as described in Fig. 1D. (E–G) Pib1, Rsp5 and Cue1 exhibit distinct E2 and linkage selectivities in polyubiquitin chain synthesis. *In vitro* ubiquitylation assays were carried out at 30°C for 60 min as described in A, using ^{His}Ubc4, Ubc7^{His} and ^{His}Ubc13–Mms2 as E2s and ^{GST}Pib1ΔFYVE, ^{GST}Rsp5 and ^{GST}Cue1^{His} as E3s, respectively. Use of mutant ubiquitin is indicated by K63R or K48R, respectively. (H) Discharge of the Ubc13-thioester is enhanced by Pib1. Ubc13(K92R) was charged with ubiquitin in the presence of E1, ATP and ubiquitin for 60 min at 30°C. Reactions were stopped by apyrase treatment, and discharge of Ubc13~Ub was initiated by the addition of lysine (for all conditions), Mms2 and Pib1-RING+100aa as indicated. Reactions were incubated at 30°C for the indicated times and analysed under non-reducing conditions unless indicated (+DTT, addition of dithiothreitol). (I) Ubc4-thioester discharge is stimulated by Rsp5, but not by Pib1. Ubc4(K91R) was charged with ubiquitin for 10 min at 30°C, and discharge of Ubc4~Ub was analysed in the presence of lysine (in all conditions) and Rsp5 or Pib1-RING+100aa as indicated, using non-reducing conditions unless otherwise noted (+DTT). Blots and gels are representative of n>2 (A–E,H,I) or n=2 (F,G) experiments performed under identical or similar conditions.

Ubc13–Mms2 colocalises with Pib1 at internal membranes

Pib1 localises to membranes of the endocytic compartment via its lipid-binding FYVE domain and accumulates at the vacuolar periphery (Burd and Emr, 1998; Shin et al., 2001). As expected, the fungal E3s featuring a genuine FYVE domain localised in a Pib1-like pattern when expressed as fusions to GFP in budding yeast (Fig. 4A). In contrast, RFFL was targeted predominantly to the plasma membrane. This is consistent with the situation in mammalian cells, where RFFL has been reported to associate with both the plasma membrane and the endocytic compartment (Coumailleau et al., 2004; McDonald and El-Deiry, 2004), and its targeting was described to be in part governed by palmitoylation (Araki et al., 2003).

Although the Ubc13–Mms2 complex is mostly distributed in the cytoplasm in a diffuse pattern, sporadic vacuole-associated Ubc13^{GFP} foci colocalising with Pib1^{mCherry} were detectable in some of the cells, consistent with an interaction of the proteins *in vivo* (Fig. 4B). Upon overexpression of Pib1^{mCherry} by means of a copper-inducible promoter, localisation of Ubc13^{GFP} to the vacuolar membrane was strongly enhanced, indicating that Pib1 is able to recruit the E2 to internal membranes (Fig. 4B,C). Consistent with the mode of E2–E3 interaction defined above (Fig. S1A), recruitment of Ubc13 required an intact Pib1 RING finger, as mutation of I227 to alanine abolished the colocalisation without affecting membrane association of Pib1 itself (Fig. 4C,D). In addition, Ubc13 recruitment was independent of Mms2 (Fig. 4E), but membrane association of Mms2 in turn required the presence of Ubc13 in this assay (Fig. 4F).

In order to evaluate the specificity of Ubc13–Mms2 recruitment, we also monitored the localisation of Ubc13^{GFP} upon overexpression of mCherry-tagged Hrd1 (Fig. 4C). Although ER association of Hrd1^{mCherry} was clearly detectable, Ubc13^{GFP} did not accumulate at this compartment (Fig. 4G). These data indicate that the complex of Ubc13–Mms2 and Pib1 as characterised in the two-hybrid screen and verified biochemically is also identifiable in the physiological environment of a cell, and that recruitment of the E2 is specific for Pib1 and the endocytic compartment.

Genetic interactions implicate Ubc13–Mms2 in membrane protein sorting

The cooperation of Ubc13–Mms2 with the membrane-associated E3s *in vitro* and their colocalisation in cells strongly suggested a functional involvement of Ubc13–Mms2 in the endocytic pathway. In order to test this hypothesis, we used analysis of genetic interaction profiles as an unbiased approach to identify gene functions (Costanzo et al., 2011). We mined a previously published genome-scale genetic interaction map (Costanzo et al., 2016) for genes whose interaction patterns resembled those of *UBC13* and *MMS2* (Table S1). This map comprises fitness measurements based on colony size for ∼23 million double-mutant combinations, covering ∼90% of budding yeast genes. In this data set, the genetic interaction profiles of *UBC13* and *MMS2* correlated not only with each other, but also – to a comparable extent – with those of various genes involved in vacuolar transport and the MVB pathway (Fig. 5A,B). Based on gene ontology (GO) term analysis, these pathways were strongly overrepresented among the most highly correlated genes for both *UBC13* and *MMS2* (Fig. 5C). In particular, numerous genes encoding components of all ESCRT complexes emerged at the top of the list (these were *HSE1* and *YNR005C*, a dubious predicted ORF overlapping with *VPS27*, for ESCRT-0; *SRN2* and *MVB12* for ESCRT-I; *VPS25* for ESCRT-II and the ESCRT-III-associated *VPS4*). Similarly, the *UBC4* interaction profile correlated with those of MVB pathway-associated genes, as expected from Ubc4's cooperation with Rsp5 (Fig. 5C). In contrast, such correlations were not found for genes encoding other E2s like *RAD6*, *UBC7* or *UBC5*, suggesting that those observed for *UBC13*, *MMS2* and *UBC4* are specific. Surprisingly, the genetic interaction profile of *PIB1* did not correlate with those of *UBC13* and *MMS2*, and although more than 20% of the top *PIB1*-correlating genes (r>0.13) encoded proteins associated with either the plasma membrane or the vacuolar compartment, no single GO term was significantly overrepresented.

Analysis of individual genetic relationships (Table S2) revealed significant negative interactions of both *ubc13Δ* and *mms2Δ* mutants with candidates that were expected based on their contribution to genome maintenance (such as *rev1Δ*, *rev3Δ*, *rev7Δ* and *pol32Δ*), but also with three different *rsp5* alleles and (for *ubc13Δ*) with *tul1Δ* (Fig. 5D,E). Thus, both genetic interaction profiles and individual genetic interactions suggested a functional role for Ubc13–Mms2 in membrane protein sorting. Although individual genetic interaction data obtained by high-throughput assays should be evaluated with care due to the potential to generate false positives, the statistical analysis as well as the overlap between *UBC13* and *MMS2* provide additional confidence, consistent with the well-established cooperation between the two proteins.

Ubc13–Mms2 contributes to membrane protein turnover via the MVB pathway

In order to directly evaluate a potential role of Ubc13–Mms2 in the endocytic pathway, we focussed on a set of membrane proteins whose trafficking has been reported to involve K63-polyubiquitylation. We first asked whether Ubc13 might cooperate with Pib1 in the modification of the v-SNARE Snc1, which was previously found to be subject to K63-linked polyubiquitylation (Xu et al., 2017). This modification was reported to mediate interactions with the COPI complex, thus

Journal of Cell Science (2020) 133, jcs244566. doi:10.1242/jcs.244566

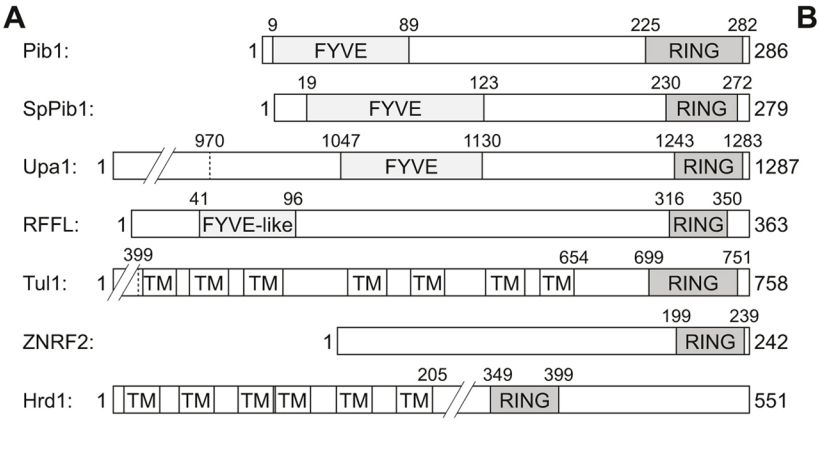

B

protein	organism	yeast E2	human E2
Pib1	*S. cerevisiae*	Ubc13 Mms2	**UBE2N,** UBE2V1, UBE2V2, UBE2W
SpPib1	*S. pombe*	**Ubc13** Mms2	**UBE2B, UBE2D1-D3, UBE2E1-E3, UBE2N, UBE2V1, UBE2V2, UBE2W**
Upa1	*U. maydis*	Ubc13	UBE2D1-D3, UBE2E1-E2, **UBE2N,** UBE2V1, UBE2V2, UBE2W
RFFL	*H. sapiens*	-	UBE2W
Tul1	*S. cerevisiae*	Ubc1, Ubc4 Ubc5, **Ubc6** Ubc13	**UBE2D1-D3, UBE2E1-E3, UBE2K,** UBE2N, UBE2V1, **UBE2W**
ZNRF2	*H. sapiens*	Ubc1	**AKTIP, UBE2D1-D3, UBE2E1-E3, UBE2N, UBE2T, UBE2V1, UBE2W**
Hrd1	*S. cerevisiae*	-	**UBE2E1-E2, UBE2N,** UBE2W

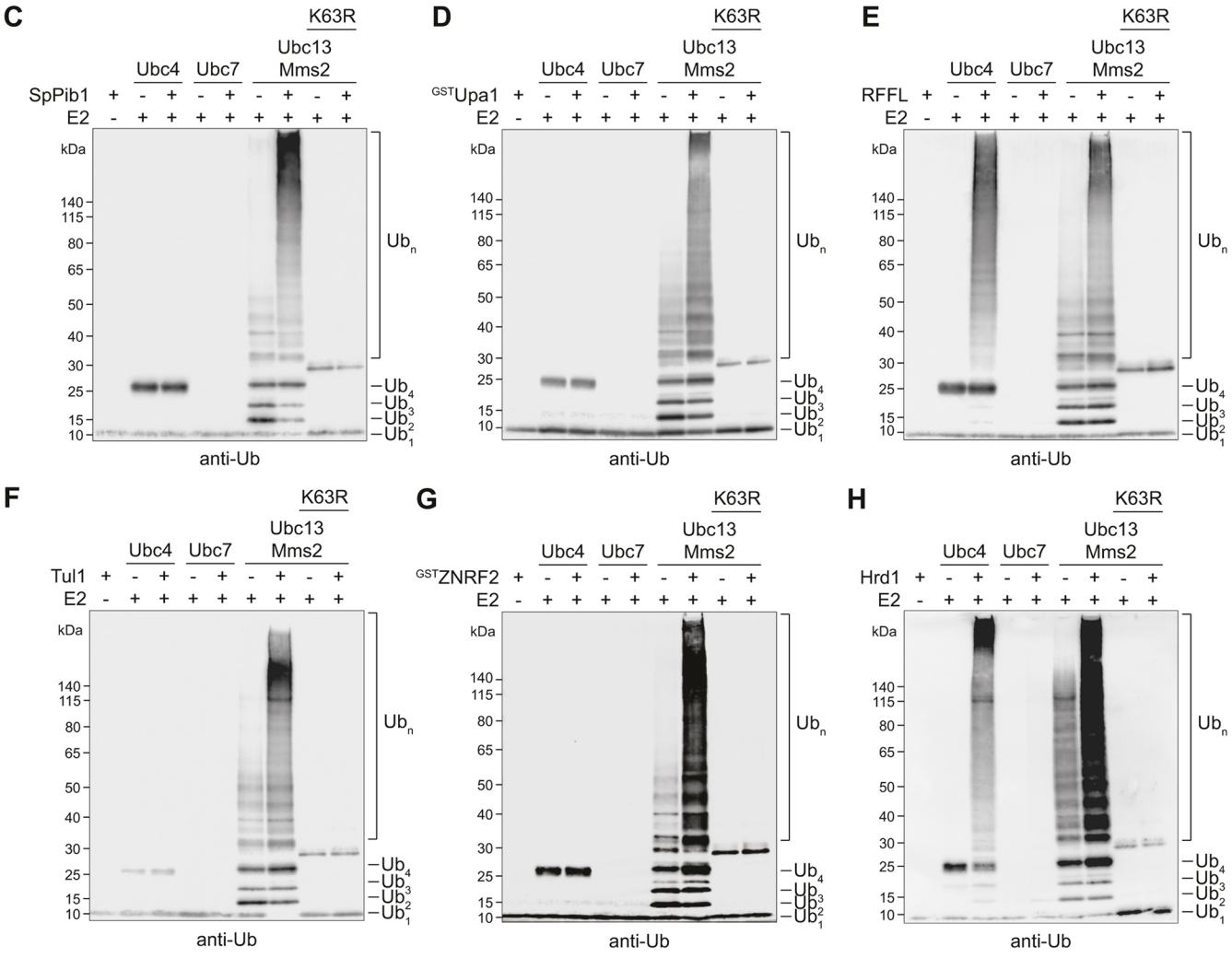

Fig. 3. Other membrane-associated RING E3s share Pib1's selectivity for Ubc13–Mms2. (A) Domain structures of the indicated membrane-associated RING E3s (TM: transmembrane domain). (B) Membrane-associated RING E3s interact with a range of budding yeast and/or human E2s in the two-hybrid assay. Strong interactions are indicated in bold. Original plates are shown in Fig. S3. (C–H) Selected RING E3s cooperate with Ubc13–Mms2 in K63-polyubiquitylation. Recombinant SpPib1(123–279) (C), ^{GST}Upa1(1131–1287) (D), RFFL(97–363) (E), Tul1(655–758) (F), ^{GST}ZNRF2 (G) and Hrd1(325–551) (H) were analysed in ubiquitin chain formation assays with the indicated recombinant E2s (see Fig. 2E–G) as described in Fig. 2A. All reactions contained E1, ATP and ubiquitin (WT or K63R) and were carried out at 30°C for 60 min. Blots shown are representative of *n*=2 experiments.

contributing to the recycling of Snc1 to its donor membranes (Xu et al., 2017). Based on the impairment of a *pib1Δ tul1Δ* double mutant in Snc1 recycling, Pib1 and Tul1 were postulated to act redundantly as E3s modifying the v-SNARE (Xu et al., 2017). Ubc13–Mms2 could thus contribute to the modification as an E2. However, although Snc1 ubiquitylation was detectable in our hands,

Journal of Cell Science (2020) 133, jcs244566. doi:10.1242/jcs.244566

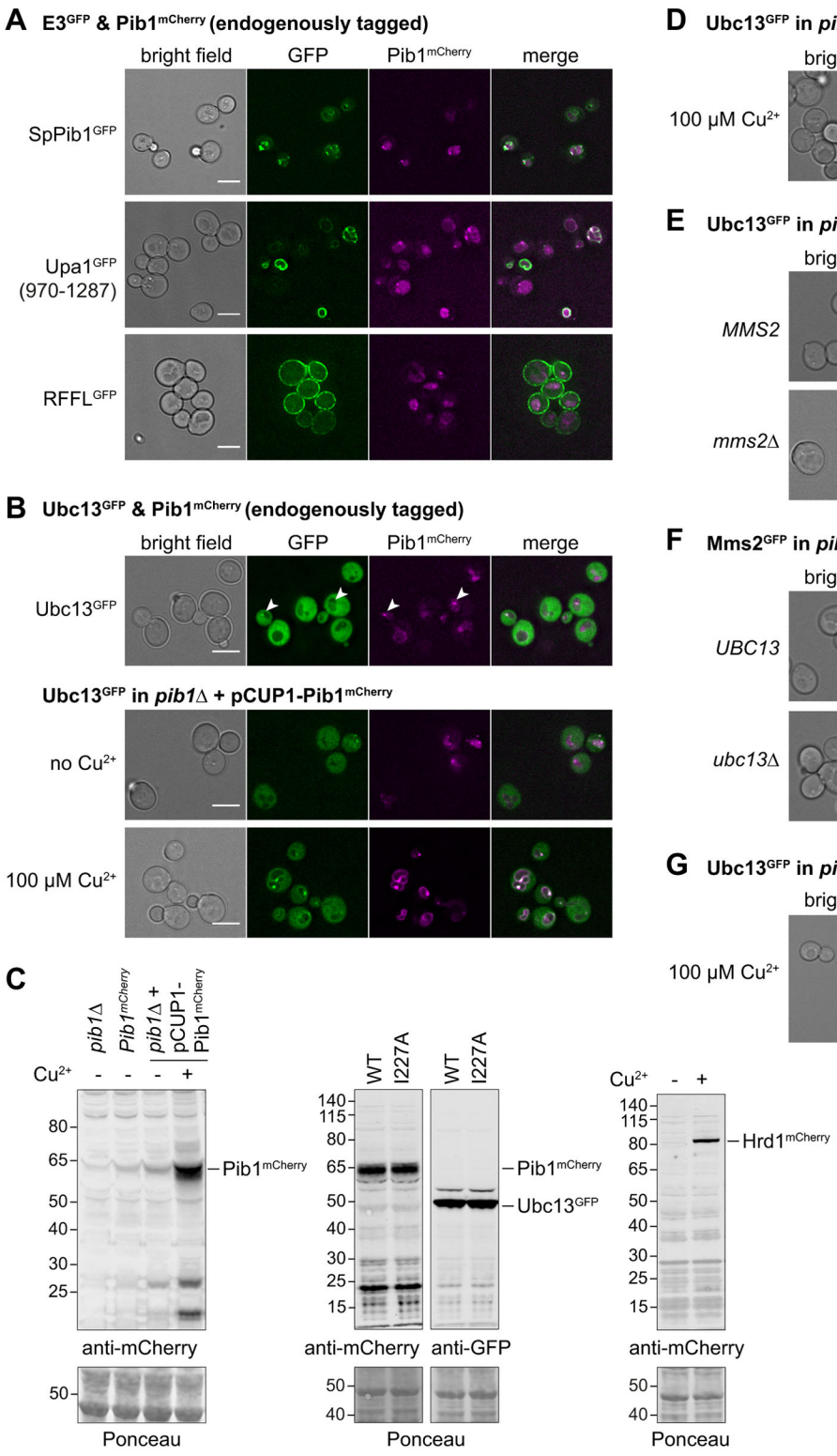

Fig. 4. See next page for legend.

the modification pattern was not altered in *ubc13Δ*, *pib1Δ*, *tul1Δ* or *pib1Δ tul1Δ* mutants (Fig. S5A). Snc1 has also been identified as a target of K63-ubiquitylation upon treatment of yeast with hydrogen peroxide in a proteomic screen (Silva and Vogel, 2015). Although Snc1 ubiquitylation levels were enhanced by addition of hydrogen peroxide, deletion of *UBC13*, *PIB1* and/or *TUL1* did not diminish them (Fig. S5B). However, the modification was completely abolished in an *rsp5* mutant (Fig. S5C). These results argue against Ubc13 acting with Pib1 and Tul1 directly on Snc1, but rather imply an indirect effect of the two E3s on Snc1 recycling or turnover.

K63-polyubiquitylation is also involved in the endocytosis of plasma membrane transporters such as the uracil permease Fur4 (Galan and Haguenauer-Tsapis, 1997). Modification of Fur4 itself

Journal of Cell Science (2020) 133, jcs244566. doi:10.1242/jcs.244566

Fig. 4. Localisation of RING E3s and Ubc13–Mms2 in budding yeast cells. (A) Selected RING E3s localise in distinct patterns in budding yeast. Cells harbouring endogenously tagged Pib1^{mCherry} and GFP-tagged E3s expressed from a centromeric plasmid under control of the *CUP1* promoter were grown in SC medium containing 70 µM $CuSO_4$ at 30°C, and images were acquired by deconvolution microsopy. (B) Pib1 recruits Ubc13 to intracellular membrane structures. Exponentially growing cultures of yeast cells expressing Ubc13^{GFP} and Pib1^{mCherry} in SC medium were imaged by deconvolution microscopy. Arrowheads highlight colocalisation of Pib1 and Ubc13. Top row: endogenously tagged Pib1^{mCherry}; middle row: Pib1^{mCherry} expressed under control of the *CUP1* promoter, in the absence of $CuSO_4$; bottom row: Pib1^{mCherry} expressed under control of the *CUP1* promoter, in the presence of 100 µM $CuSO_4$. (C) Verification of protein levels by western blotting. Left: Pib1^{mCherry} protein levels in the strains used in B, along with *pib1Δ* harbouring Ubc13^{GFP}, in the presence or absence of 100 µM $CuSO_4$ as indicated (Cu^{2+}). Middle: Pib1^{mCherry} and Ubc13^{GFP} protein levels in the strains used in D. Right: Hrd1^{mCherry} protein levels in the presence or absence of 100 µM $CuSO_4$ in the strain used in G. Ponceau stain images show protein loading. (D) Mutation of the Pib1 RING finger abolishes recruitment of Ubc13^{GFP} to membrane structures. Localisation assays were performed as described in B. (E) Deletion of *MMS2* has no effect on membrane recruitment of Ubc13^{GFP} by Pib1^{mCherry}. (F) Deletion of *UBC13* abolishes membrane recruitment of Mms2^{GFP} by Pib1^{mCherry}. (G) Overexpression of Hrd1^{mCherry} has no effect on the localisation of Ubc13^{GFP}. For A,B,D–G, single deconvolved *z*-planes are shown, representative of *n*=3 (A,B) or *n*=2 (D–G) experiments. Scale bar: 5 µm. For C, expression control by western blotting was performed once for each experiment.

is mediated by Rsp5 (Galan et al., 1996), but other ligases, including Pib1, contribute to cargo delivery to the vacuole via the MVB pathway (Nikko and Pelham, 2009). When we monitored endocytosis of Fur4 by uracil uptake assays after cycloheximide treatment (Volland et al., 1994), we observed delays in both *ubc13Δ* and *mms2Δ* mutants (Fig. 6A). Fur4 ubiquitylation was unaffected in *ubc13Δ* and *pib1Δ* mutants, suggesting that the permease is not a direct target of this E2–E3 pair (Fig. 6B). In the MVB pathway, Pib1 acts redundantly with an endosomal Rsp5 adaptor, Bsd2, which facilitates transport of endocytic vesicles from the Golgi to the vacuole (Nikko and Pelham, 2009). In consequence, Fur4 is successfully internalised in *bsd2Δ pib1Δ* double mutants, but accumulates in endosomes and fails to be degraded in the vacuole. In order to determine the step at which Ubc13–Mms2 participates in Fur4 turnover, we employed fluorescence microscopy to monitor the localisation of GFP-tagged Fur4 after inducing endocytosis by means of cycloheximide treatment in a *bsd2Δ* background. We found that deletion of *UBC13*, like deletion of *PIB1*, did not prevent Fur4 internalisation, but caused its accumulation in internal vesicles (Fig. 6C). Colocalisation with mCherry-tagged Vph1, a subunit of the vacuolar ATPase, confirmed that these vesicles were predominantly situated at the vacuolar periphery (Fig. S5D). Residual GFP signal in the vacuole of *bsd2Δ pib1Δ*, but not *bsd2Δ ubc13Δ*, suggested a stronger defect in Ubc13- compared to Pib1-deficient cells.

If Ubc13–Mms2 cooperates with Pib1 in the MVB pathway, then *ubc13* and *pib1* mutations should behave epistatically with respect to Fur4 degradation in a *bsd2Δ* background. In order to assess this quantitatively, we made use of the fact that the GFP moiety of Fur4^{GFP} is resistant to proteolysis and transiently accumulates in the vacuole (Nikko and Pelham, 2009). This allows for the monitoring of free GFP as a reporter for vacuolar delivery. A *doa4Δ* mutant was used as a control because it was previously shown to be completely defective in Fur4 internalisation and vacuolar targeting (Galan and Haguenauer-Tsapis, 1997). As reported previously (Nikko and Pelham, 2009), deletion of *PIB1* alone had no effect, but did impede Fur4^{GFP} degradation in a *bsd2Δ* background (Fig. 6D,E, Fig. S5E). The *ubc13Δ* mutant exhibited a phenotype similar and additive to that of *bsd2Δ*. Importantly, *pib1Δ* did not significantly enhance the *ubc13Δ* phenotype, either alone or in combination with *bsd2Δ*. This implies that Ubc13–Mms2 cooperates with Pib1 in vacuolar delivery of Fur4. The defect of the *ubc13Δ* single mutant suggests that the E2 fulfils additional roles in membrane trafficking not shared by Pib1 or Bsd2. The *tul1Δ* mutant or combinations of *tul1Δ* with *bsd2Δ* or *pib1Δ* were not impaired in Fur4 degradation, indicating that Tul1 does not functionally overlap with Pib1 in Fur4 turnover (Fig. S5F).

In order to assess whether the activity of Ubc13–Mms2 extended to other endocytic cargo proteins, we characterised the cadmium-induced vacuolar delivery of the metal transporter Smf1, which was reported to also involve Bsd2 and Pib1 (Nikko and Pelham, 2009). Consistent with a contribution of Ubc13–Mms2, ^{GFP}Smf1 accumulated in vesicles and at the vacuolar periphery in *bsd2Δ ubc13Δ* and *bsd2Δ mms2Δ* double mutants (Fig. 7).

Thus, consistent with the genetic interaction data (Fig. 5), Ubc13-mediated ubiquitylation appears to exert an effect on the endocytic system at the stage of vacuolar delivery of endocytic vesicles via the MVB pathway. In this context the E2 cooperates with Pib1, but our data suggest additional, Pib1-independent activities that might reflect a cooperation with other E3s. This function of Ubc13–Mms2 is distinct from that of Rsp5, but is important for the turnover of plasma membrane proteins like Fur4 and Smf1. In conclusion, our observations suggest that K63-polyubiquitylation in the endocytic compartment is mediated not exclusively by Rsp5, but also by Ubc13–Mms2.

DISCUSSION

Contribution of Ubc13–Mms2 to K63-polyubiquitylation at internal membranes

Polyubiquitin chains of K63-linkage have been implicated in many aspects of membrane trafficking (Erpapazoglou et al., 2014). In budding yeast, Rsp5 has so far been the only verified source of that chain type within the cytoplasmic compartment. Our results show that Ubc13–Mms2, aided by the RING E3 Pib1 and potentially other membrane-associated E3s, contributes to protein sorting in the MVB pathway, thus expanding the scope of this E2 beyond its known nuclear function with Rad5 in genome maintenance.

Recombinant Pib1 was previously reported to cooperate *in vitro* with a highly non-selective E2, UBCH5A (Shin et al., 2001), which is not known for a particular bias towards the K63-linkage. Our results indicate a clear preference of Pib1 for Ubc13–Mms2, thus strongly implicating this E2–E3 pair in the formation of K63-chains at internal membranes. An earlier claim regarding K63-specificity of Pib1 was made by Xu et al. (2017), who observed a redundant function of Pib1 and Tul1 in COPI-mediated vesicle sorting. They found that an interaction of the COPI complex with a ubiquitylated v-SNARE, Snc1, mediated by K63-selective ubiquitin binding, drives the recycling of the v-SNARE to its donor membranes. Deletion of *PIB1* and *TUL1* inhibited Snc1 recycling, and fusion of a non-specific deubiquitylating enzyme (DUB) to Pib1 or Tul1 interfered with Snc1 ubiquitylation and trafficking (Xu et al., 2017). From these indirect data they concluded that Pib1 – together with Tul1 – acts as a cognate E3 in K63-ubiquitylation of Snc1. However, by direct observation of its modification pattern, we found no defect in Snc1 ubiquitylation in the *pib1Δ tul1Δ* mutant, which suggests an indirect effect of the ligases on vesicle trafficking rather than an involvement in ubiquitin conjugation to the v-SNARE. The observed dominant negative effects exerted by the E3–DUB fusions could be attributable to a physical proximity of the ligases to Snc1,

Journal of Cell Science (2020) 133, jcs244566. doi:10.1242/jcs.244566

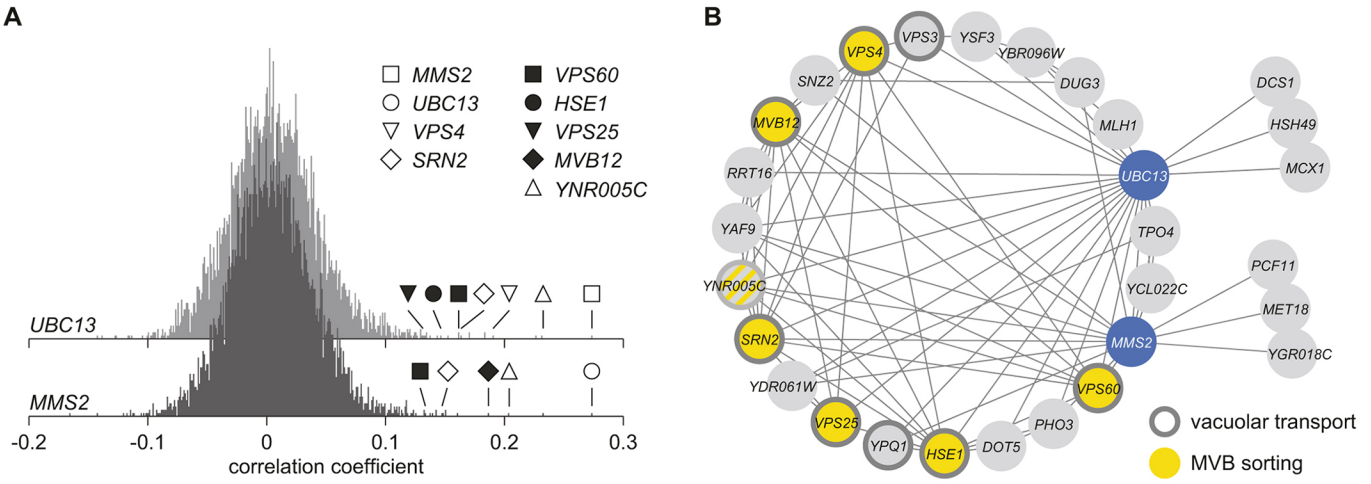

C

GO term	gene	p value	fraction (r > 0.13)	fraction (whole data set)
vacuolar transport (0007034)	*UBC13* *MMS2*	6.26e-05 0.04547	31.8% 25.0%	2.3%
MVB pathway (0071985)	*UBC13* *MMS2*	0.0045 0.03255	18.2% 18.8%	0.8%
ubiquitin / MVB (0043162)	*UBC4*	0.00023	10.5%	0.5%

D

Gene	score (*ubc13*)	p value	score (*mms2*)	p value
□ *rev1*	-0.3201 -0.1389	2.067E-33 7.485E-6	-0.3956 -0.2900	0.0001141 0.003044
○ *rev3*	-0.1689 -0.1172	0.01855 6.119E-49	-0.3379 -0.1501	0.007345 0.0000
▽ *rev7*	-0.3186 -0.0432	3.316E-12 n.s.	-0.1823 -0.0750	0.001768 2.899E08
◇ *pol32*	-0.2630 -0.1734	1.945E-5 4.728E-6	-0.1694 -0.1343	0.006305 3.176E014
■ *rsp5-1*	-0.2347	0.001386	-0.1326 -0.0446	1.31E-5 0.0003561
● *rsp5-3*	-0.1453	0.003903	-0.1474 -0.0806	0.02657 8.114E-6
▼ *rsp5-sm1*	-0.0745	n.s.	-0.1851 -0.1193	1.866E-5 n.s.
◆ *tul1*	-0.2702 0.0198	0.009492 n.s.	-0.0029	n.s.

E

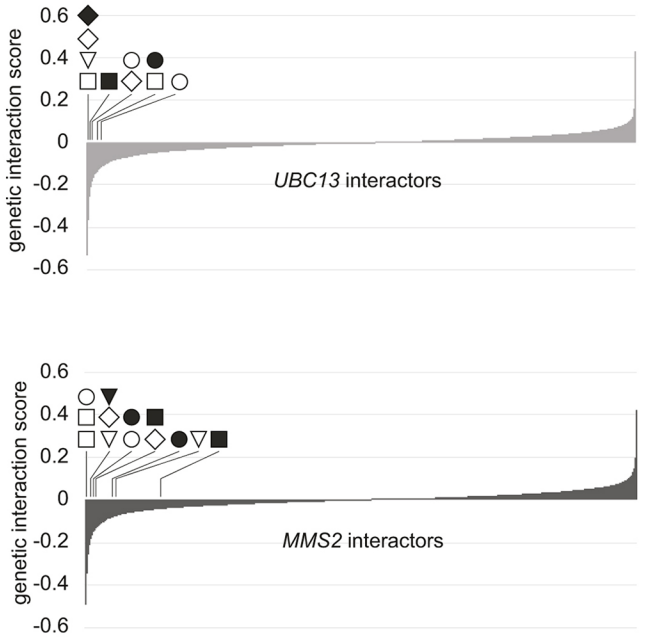

Fig. 5. Genetic interactions implicate *UBC13* and *MMS2* in membrane protein sorting. (A) Functional similarity between *UBC13*, *MMS2* and components of membrane protein sorting pathways. Histograms of Pearson correlation coefficients calculated between the genetic interaction profiles of *UBC13* and *MMS2* and ∼90% of all yeast genes are shown, obtained from a previously published genome-scale genetic interaction map (Costanzo et al., 2016). All interactions included in the analysis are shown in Table S1. (B,C) Genes involved in vacuolar transport and the MVB pathway are overrepresented among those whose interaction profiles most strongly correlate with *UBC13* and *MMS2* (Pearson correlation coefficient >0.13). The network of genes correlating with *UBC13* or *MMS2* is shown in B. All correlations within the group above the 0.13 threshold are shown. Genes involved in vacuolar transport (gene ontology term GO: 0007034) and the MVB sorting pathway (GO: 0071985) are highlighted. Note that *YNR005C* is a dubious ORF overlapping with *VPS27*. The fraction of genes with relevant GO terms among those depicted in B versus the total fraction of genes with these GO terms in the data set is shown in C. Significance is indicated by *P*-values. A corresponding analysis for *UBC4* is shown for comparison. (D,E) *UBC13* and *MMS2* exhibit negative genetic interactions with genes involved in translesion synthesis and membrane protein sorting. Genetic interaction scores of *UBC13* and *MMS2* with relevant genes are shown in D, obtained from the same genetic interaction map as in A (Table S2). Significance is indicated by *P*-values (ns, not significant; *P*>0.05). Note that two interaction scores are provided for some combinations, based on the availability of query and array alleles in the library. Plots of all genetic interaction scores for *UBC13* and *MMS2* are shown in E. Symbols indicate significant interactors from D.

mediated by the membrane association of the E3s, but they do not prove an enzyme-substrate relationship.

Our findings provide conclusive evidence for a cooperation of Ubc13–Mms2 with Pib1, and possibly with additional E3s, in K63-polyubiquitylation at endosomal and vacuolar membranes. However, several attempts using proteomic analysis and two-hybrid screens have failed to reveal any direct physiological substrates of Ubc13–Mms2 or Pib1 in our hands (C.R., V.T., T.K.A. and H.D.U. unpublished). One possible reason for this failure might be a high degree of redundancy between the ubiquitin conjugation factors

Journal of Cell Science (2020) 133, jcs244566. doi:10.1242/jcs.244566

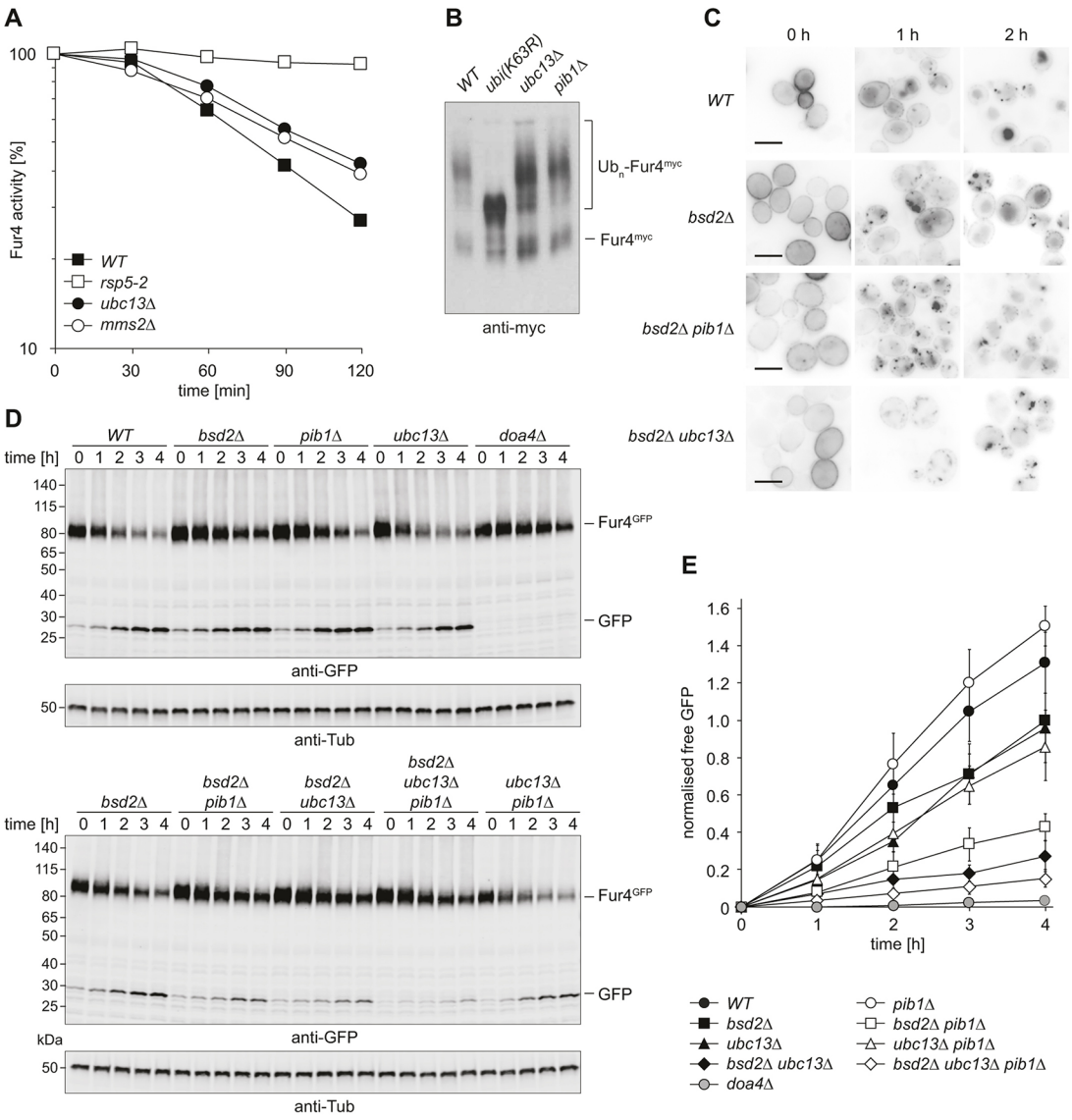

Fig. 6. Ubc13–Mms2 contributes to membrane protein sorting. (A) Internalisation of Fur4 is delayed in *ubc13Δ* and *mms2Δ*. Fur4^{myc} was overexpressed from a multicopy plasmid, and internalisation of the permease was induced by addition of 100 µg ml^{-1} cycloheximide. The amount remaining at the plasma membrane at the indicated time points was quantified relative to t=0 by uracil uptake assays. A temperature-sensitive *rsp5* mutant served for comparison. Data are representative of *n*>3 independent experiments. (B) Fur4 polyubiquitylation is not dependent on *UBC13* or *PIB1*. Fur4^{myc} was expressed in the indicated strains from a multicopy plasmid, and the protein was detected by western blotting of a membrane-enriched lysate with an anti-myc antibody. Blots are representative of *n*=3 experiments. (C) Fur4 delivery to the vacuole is blocked by deletion of *UBC13* in a *bsd2Δ* background. Localisation of FUR4^{GFP} in the indicated strains was tracked by fluorescence microscopy at the indicated time points after induction of endocytosis by addition of 100 µg ml^{-1} cycloheximide. Scale bars: 5 µm. Images representative of *n*=3 experiments are shown. (D) Pib1 and Ubc13 cooperate in the delivery of Fur4 to the vacuole. Internalisation of Fur4^{GFP}, expressed from a centromeric plasmid under control of a *GAL1* promoter, was induced in strains of the indicated backgrounds by addition of 100 µg ml^{-1} cycloheximide. Samples were taken at the indicated times, and total cell extracts were analysed by western blotting with anti-GFP and anti-α-tubulin antibodies. (E) Quantification of vacuolar degradation of Fur4^{GFP}. Accumulation of free GFP on the blots shown in D was plotted relative to the GFP signal at 4 h in *bsd2Δ*. Data are mean±s.d. of *n*=3 independent experiments, each performed in technical duplicate. The α-tubulin signal was used as a loading control. A statistical analysis is shown in Fig. S5E. For details, see Materials and Methods.

involved in the endocytic pathway, as emerging information about E3s such as Rsp5, Pib1 and Tul1 suggests that they might be able to compensate for each other to some degree (Nikko and Pelham, 2009). Moreover, it is well established that delivery of membrane proteins to the vacuole requires multiple ubiquitylation events at various stages and on many different targets, not limited to the cargo proteins themselves. Redundancy between membrane-associated E3s also provides a likely explanation for the lack of a detectable phenotype of the *pib1Δ* single mutant and thus the absence of any GO term enrichment in its genetic interaction profile.

Finally, the marked preference of Ubc13–Mms2 for K63 of ubiquitin could indicate a predominant function in chain elongation rather than *de novo* modification of specific substrates. This is the case for Ubc13–Mms2 in cooperation with Rad5 (Hoege et al., 2002; Ulrich and Jentsch, 2000), and the exquisite specificity of Pib1 for Ubc13–Mms2 could indicate a similar phenomenon.

Selectivity of E2–E3 pairing in membrane protein sorting

Our identification of budding yeast Pib1 as an E3 with an unusually high preference for the K63-specific Ubc13–Mms2 complex raises

Journal of Cell Science (2020) 133, jcs244566. doi:10.1242/jcs.244566

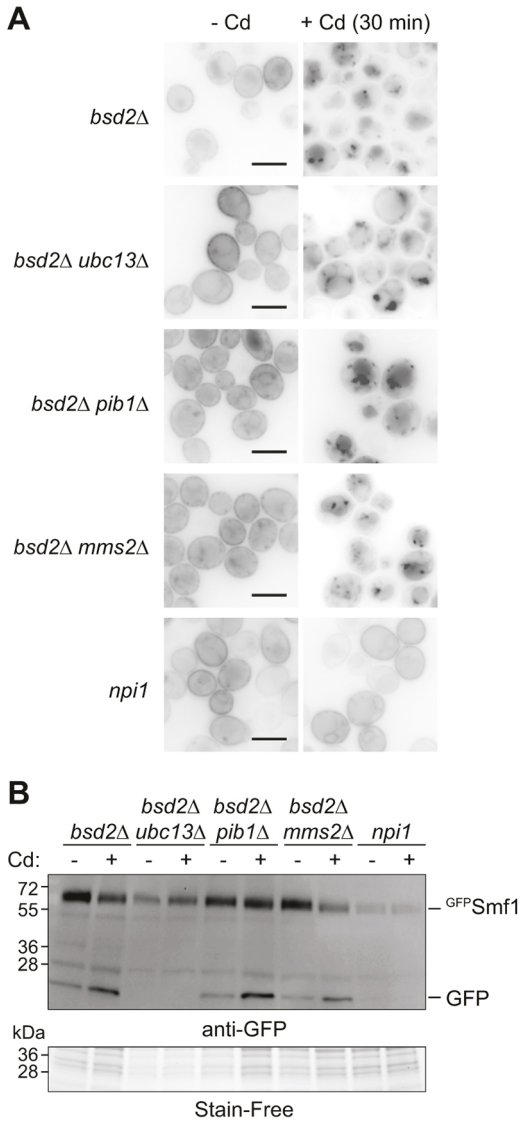

Fig. 7. Ubc13–Mms2 contributes to the delivery of the metal transporter Smf1 to the vacuole. (A) Localisation of ^{GFP}Smf1, expressed from a centromeric plasmid in the indicated mutants, was followed by fluorescence microscopy before and 30 min after induction of transporter endocytosis by addition of 2 µM $CdSO_4$ to exponentially growing cultures. The *RSP5* mutant *npi1* was used as a control strain defective in the internalisation step. Scale bars: 5 µm. Images shown are representative of $n>2$ experiments. (B) Emergence of free GFP as a sign of delivery of ^{GFP}Smf1 to the vacuole was monitored by western blotting in the indicated strains. Loading is indicated by Stain-Free image. Blots shown are representative of $n=2$ experiments.

a general question about the origin of selectivity in E2–E3 cooperation. Based on sequence or structural information alone, predictions about productive pairings have not yet been successful, necessitating a combination of biochemical and functional experiments to determine physiological pairs. This necessity is illustrated by our observation that Hrd1 strongly stimulated Ubc13–Mms2 and Ubc4 *in vitro*, although this E3 is highly selective for Ubc7 in the ER-associated protein degradation (ERAD) pathway (Bays et al., 2001). In that context, Hrd1 is assisted by the Ubc7-interacting co-factor Cue1 (Biederer et al., 1997), which explains its poor activity with Ubc7 in assays where Cue1 is not present (Fig. 3H, Fig. S4A).

Within the endocytic compartment, the reported colocalisation and redundancy between Pib1 and Tul1, along with our *in vitro* activity assays, suggest that Tul1 – like Pib1 – cooperates with Ubc13–Mms2 in K63-ubiquitylation. Yet, the protein was originally described to interact with Ubc4 (Reggiori and Pelham, 2002). Although we were unable to reproduce this finding or detect any catalytic activity with yeast Ubc4, our interaction and activity assays suggest that Tul1 might be less selective than Pib1.

Ubc13–Mms2 was also found to be active with a family of related E3s from other species, all harbouring a lipid-binding FYVE- or FYVE-like domain in addition to the RING finger. Interestingly, while they all supported Ubc13–Mms2 activity, the scope of their interactions and activities with other E2s varies considerably. The putative Pib1 homologue from *S. pombe*, SpPib1, displayed an identical localisation and a very similar activity pattern, although its interactions in the two-hybrid system were less selective than those of budding yeast Pib1. Given its preference for Ubc13, it is surprising that SpPib1 was reported to target a subunit of the exocyst, Sec3, for proteasomal degradation (Kampmeyer et al., 2017), a process usually associated with K48-linked polyubiquitylation. However, a degree of redundancy between Pib1 and other E3s (including Rsp5) was noted in that study, and a contribution of vacuolar degradation was not rigorously excluded, thus leaving open the possibility that multiple degradation systems act on Sec3. *U. maydis* Upa1 closely resembled budding yeast Pib1 with respect to localisation, E2 binding and E2 activation, implying a similarly Ubc13-selective function. Interestingly, the protein bears a large N-terminal extension, including a motif for interaction with the key RNA transport protein Rrm4, which implicates Upa1 in vesicle-mediated long-distance transport of mRNP particles (Pohlmann et al., 2015). Thus, the protein appears to couple endosome dynamics with RNA transport.

RFFL (also known as CARP2 or Sakura) displayed the lowest selectivity among the FYVE-type E3s. Accordingly, the protein has been reported to modify a diverse set of substrates, many of them localising to the plasma membrane or endocytic vesicles (Araki et al., 2003; Liao et al., 2008; McDonald and El-Deiry, 2004; Okiyoneda et al., 2018). RFFL was often observed to act redundantly with a closely related protein, RNF34 (also called CARP1 or Momo) (Araki et al., 2003; Liao et al., 2008). Whereas most instances of RFFL- and RNF34-mediated ubiquitylation appear to involve proteasomal degradation (Araki et al., 2003; Liao et al., 2009, 2008; McDonald and El-Deiry, 2004; Wei et al., 2012; Yang et al., 2007; Zhang et al., 2014), there are cases where a contribution of lysosomal proteolysis has been demonstrated (Jin et al., 2014; Okiyoneda et al., 2018). For example, in a recent report, RFFL was shown to mediate retrieval from the plasma membrane and subsequent lysosomal degradation of a non-native CFTR mutant via interaction and K63-polyubiquitylation in a post-Golgi compartment (Okiyoneda et al., 2018). In this context, cooperation with UBC13 appears plausible.

In conclusion, our data point to the existence of a conserved group of membrane-associated RING E3s that can cooperate with Ubc13–Mms2 in the generation of K63-linked polyubiquitin chains and contribute to protein sorting in the endocytic and MVB pathways. The molecular features determining their selectivity, as well as the relevant targets of ubiquitylation, remain to be explored.

MATERIALS AND METHODS

Yeast strains, plasmids and antibodies

All yeast strains used in this study are listed in Table S3. Single gene deletions in the BY4741 background were obtained from the yeast knockout collection (Dharmacon). Other gene deletions were generated by PCR-based

Journal of Cell Science (2020) 133, jcs244566. doi:10.1242/jcs.244566

methods (Janke et al., 2004) or genetic crosses. The *npi1* strain, carrying a *KanMX* cassette within the *RSP5* promoter, was a gift from Bruno André (Université Libre de Bruxelles, Faculté des Sciences, Belgium). Tagging of Pib1, Ubc13, Mms2 and Vph1 at their endogenous loci was achieved by recombination-mediated integration of PCR-amplified cassettes (Janke et al., 2004). Yeast strains were grown in YPD or, if selecting for maintenance of centromeric or 2 µ plasmids, synthetic complete (SC) medium lacking the appropriate amino acids [2% glucose unless otherwise noted, 6.7 g l^{-1} yeast nitrogen base without amino acids (Sigma Aldrich), 86 mg l^{-1} myo-inositol, 86 mg l^{-1} uracil, 21 mg l^{-1} adenine, 8.6 mg l^{-1} p-aminobenzoic acid and 86 mg l^{-1} of each of the 20 biogenic amino acids except lysine (172 mg l^{-1}) and those specified for selection].

All plasmids are listed in Table S4. For Fur4 endocytosis assays, $Fur4^{GFP}$ was expressed under control of a *GAL1* promoter from a centromeric vector based on YCplac33 (Gietz and Sugino, 1988). For uracil uptake assays and visualisation of Fur4 ubiquitylation, myc-tagged Fur4 was expressed under control of its own promoter from a 2 µ vector, YEplac195 (Gietz and Sugino, 1988). Two-hybrid plasmids were based on pGBT9 (Clontech) or the pGAD-C- and pGBD-C-series, expressing candidates as fusions to the Gal4 activation domain (GAD) or DNA-binding domain (GBD) and carrying the *LEU2* and *TRP1* markers, respectively (James et al., 1996). For localisation studies of Pib1 orthologues, the corresponding genes were cloned in frame with yeGFP under control of a *CUP1* promoter into a YCplac33-based centromeric plasmid. Overexpression of mCherry-tagged *HRD1*, *PIB1* and its RING finger mutant was achieved in the same manner. Plasmids for expression of ^{3HA}*SNC1* and ^{3HA}*SNC1(8KR)* under control of the *TPI1* promoter in budding yeast were kindly provided by Todd Graham (Xu et al., 2017). Point mutations were created by PCR-based mutagenesis. All antibodies are listed with their sources and dilutions where appropriate in the following sections. All have been extensively validated in this and other labs.

Yeast two-hybrid assays

The initial two-hybrid screen for interactors of Mms2 was performed with a histidine- and adenine-responsive reporter strain, PJ69-4a, and a set of three yeast genomic libraries kindly provided by Philip James (James et al., 1996). These libraries, constructed in the pGAD-C vector series representing all 3 reading frames, were amplified in *E. coli*, yielding between 80 and 200 million clones, and used in parallel for transformation of PJ69-4a expressing GBD-Mms2 from a bait plasmid carrying the *URA3* marker. Approximately 5 million clones per library were screened on SC $Ura^{-}Leu^{-}His^{-}$ selective medium. False positives were eliminated by excluding clones that allowed reporter-dependent growth without the bait plasmid, and genuine interactors were subsequently identified by plasmid isolation and sequencing after re-streaking single colonies.

Individual two-hybrid assays were performed in the haploid strain PJ69-4a as described previously (James et al., 1996). The screen for identifying E2–E3 interaction pairs was performed in a semi-automated manner in a 16×24 spot array format, using a ROTOR HDA pinning robot (Singer Instruments) with a collection of 30 human E2s, a kind gift from Rachel Klevit (Christensen and Klevit, 2009) and all yeast E2s in pGAD vectors. Open reading frames of budding yeast Pib1, human RFFL (isoform 1, from HeLa cDNA), *S. pombe* Pib1 (amino acids 123–279), *U. maydis* Upa1 (amino acids 970–1287), Tul1 (amino acids 655–758) and Hrd1 (amino acids 325–551) were PCR-amplified and cloned into pGBD-C1. Human ZNRF2 was obtained from the ORFeome clone collection (ID 47920) and transferred by Gateway cloning into pGBT9-GW (Clontech). GAD-E2 and GBD-E3 constructs were combined by transformation into PJ69-4α and PJ69-4a, respectively, and subsequent mating. The diploids were then subjected to standard two-hybrid analysis by pinning onto SC $Leu^{-}Trp^{-}$, SC $Leu^{-}Trp^{-}His^{-}$ and SC $Leu^{-}Trp^{-}His^{-}Ade^{-}$ plates. To reduce background growth, the SC $Leu^{-}Trp^{-}His^{-}$ plate was re-pinned once onto the same medium. For analysing interactions between Pib1 and the yeast E2s, this screen was repeated in the opposite direction, swapping GAD and GBD.

Protein purification

Recombinant proteins were produced in *E. coli*. Expression and purification conditions for all recombinant proteins are listed in Table S5. Briefly, His_6- and GST-tagged proteins were affinity-purified in batch on Ni-NTA agarose (Qiagen) and glutathione Sepharose 4 Fast Flow (GE Healthcare), respectively. Protease cleavage (PreScission, GE Healthcare; TEV-Protease, Biomol) was performed overnight at 4°C. Subsequent purification steps were carried out on an NGC chromatography system (Bio-Rad). Bovine ubiquitin (Ub) was purchased from Sigma-Aldrich and Ub(K6R) from Boston Biochem. ^{His}Uba1 (from mouse) and other ubiquitin variants were purified as described previously (Carvalho et al., 2012; Pickart and Raasi, 2005). ^{GST}Cue1^{His} and Hrd1 were purified as described before (Bagola et al., 2013) with some modifications.

In vitro protein–protein interaction assays

In vitro interaction studies were carried out in a buffer containing 50 mM potassium phosphate, pH 6.0, 150 mM KCl, 10% glycerol, 0.1% Triton X-100 and 1 mM dithiothreitol (DTT). Purified GST and ^{GST}Pib1ΔFYVE (100 pmol) were immobilised on glutathione Sepharose 4 Fast Flow (25 µl slurry, GE Healthcare). Beads were pre-treated with 1 mg ml^{-1} bovine serum albumin (Sigma), washed and incubated with 100 pmol His_6-tagged E2s at 4°C for 120 min. After washing the beads, bound proteins were eluted by boiling in NuPage LDS sample buffer (Thermo Fisher) supplemented with 25 mM DTT for 10 min at 95°C, and the eluate was analysed by SDS–PAGE and western blotting with anti-His_6-tag antibody (Sigma H1029, 1:5000).

Ubiquitin chain formation assays

Free ubiquitin chain formation was assayed in reactions containing 40 mM HEPES, pH 7.4, 8 mM magnesium acetate, 50 mM NaCl, 5 µM purified bovine ubiquitin (Sigma) or ubiquitin variants, 50 nM ^{His}Uba1, 30 µM ATP, 2 µM E2 and 0.5 µM E3. Reactions were incubated for 30 min (Pib1) or 60 min (other E3s) at 30°C (yeast E3s) or 37°C (human E3s), stopped by addition of NuPage LDS sample buffer supplemented with DTT, and analysed by SDS–PAGE and western blotting with a monoclonal anti-ubiquitin antibody, P4D1 (Cell Signaling Technology #3936, 1:1000). For subsequent treatment with AMSH (McCullough et al., 2004), the ubiquitylation reaction was terminated by addition of 1 unit of apyrase (New England Biolabs) per 100 µl reaction and incubation at 30°C for 15 min. This reaction was then further incubated in the presence or absence of 2 µM ^{GST}AMSH at 37°C for up to 60 min.

E2 thioester discharge assays

Ubc13(K92R) was charged with ubiquitin for 60 min at 30°C in a reaction containing 40 mM HEPES, pH 7.4, 2 mM $MgCl_2$ 50 mM NaCl, 240 nM His_6-E1, 30 µM Ubc13(K92R), 24 µM ubiquitin and 200 µM ATP. The reaction was stopped by addition of 1 unit of apyrase (New England Biolabs) per 100 µl reaction volume and incubation at 30°C for 10 min (the reaction at this stage was used as sample t=0). The reaction, now containing the Ubc13~Ub thioester, was mixed with a solution containing L-lysine (adjusted to pH 7.0; Sigma) as well as Mms2 and Pib1-RING+100aa where indicated. Final concentrations were 15 µM Ubc13/Ubc13~Ub, 15 µM Mms2, 1.5 µM Pib1-RING+100aa, 12 µM ubiquitin and 45 mM L-lysine. Reactions were incubated at 30°C for the indicated times, stopped by addition of NuPage LDS sample buffer without DTT and separated by SDS–PAGE, followed by staining with Instant Blue (Expedeon). Ubc4(K91R) was charged with ubiquitin under identical conditions at 30°C for 10 min, and lysine discharge assays were performed with 1.5 µM Pib1-RING+100aa or Rsp5 at a final concentration of 5 mM L-lysine.

E2 and E3 localisation by fluorescence microscopy

Fluorescence microscopy images were acquired with a DeltaVision Elite system (softWoRX 6.5.2) equipped with a 60× objective (NA 1.42) and a DV Elite sCMOS camera (GE Healthcare). Cells were grown to exponential phase and visualised without fixation. Images were deconvolved with softWoRx version 6.5.2 (GE Healthcare) and processed with FIJI (Schindelin et al., 2012).

Endocytosis and vacuolar delivery assays

Fur4 internalisation was measured by uracil uptake assays as described previously (Galan and Haguenauer-Tsapis, 1997; Volland et al., 1994). Briefly, exponential cultures of the relevant strains expressing $Fur4^{myc}$ from

a multicopy plasmid, grown in SC Ura$^-$ medium, were treated with 100 µg ml^{-1} cycloheximide. At the indicated time points, 1 ml aliquots were incubated with 5 µM [^{14}C]uracil for 20 s at 30°C and filtered immediately through Whatman GF/C filters. Filters were then washed twice with ice-cold water and subjected to scintillation counting. The amount of radiation taken up at each time point was plotted relative to the value at t=0. No technical replicates were performed, but the entire assay was repeated independently at least three times with comparable results, and a representative data set is shown in Fig. 6A.

Microscopic analysis of Fur4 endocytosis was performed by growing relevant strains harbouring YCplac33-GAL-Fur4-GFP overnight in SC Ura$^-$ medium containing 2% raffinose to an OD_{600} of 0.5. Expression of Fur4^{GFP} was induced by addition of 2% galactose. After 2 h, 2% glucose were added, and incubation was continued for 30 min. Endocytosis was triggered by addition of 100 µg ml^{-1} cycloheximide, and aliquots were collected for microscopy at the specified times. Smf1 endocytosis was analysed in strains harbouring plasmid pRS416-ADH-GFP-Smf1 by growing cultures in SC Ura$^-$ medium to exponential phase and addition of $CdSO_4$ for 30 min. Cells were mounted in SC medium and observed at room temperature with a motorised fluorescence microscope (model BX-61; Olympus) equipped with a Plan-Apochromat 100× oil-immersion objective (1.40 NA; Olympus), a Spot 4.05 charge-coupled device camera, and the MetaVue acquisition software (Molecular Devices). Images were processed using ImageJ (NIH, Bethesda, MD).

Delivery of Fur4 to the vacuole was assayed as described previously (Nikko and Pelham, 2009). Briefly, yeast cells harbouring YCplac33-GAL-Fur4-GFP were grown to exponential phase (OD_{600} 0.3–0.4) in SC Ura$^-$ containing 2% raffinose and 0.2% glucose, then shifted to medium containing 2% galactose and 0.1% glucose. After 2.5 h, 2% glucose was added to stop Fur4^{GFP} expression, and endocytosis was induced by addition of 100 µg ml^{-1} cycloheximide. Samples were collected at the indicated time points and flash-frozen on dry ice. Total cell extracts were prepared by trichloroacetic acid (TCA) precipitation as described previously (Morawska and Ulrich, 2013) with some modifications: precipitation was performed directly in SC medium without pelleting the cells, and the final pellet was resuspended in NuPage LDS sample buffer supplemented with 25 mM DTT and incubated for 20 min at 30°C. Samples were analysed by SDS–PAGE followed by western blotting with mouse anti-GFP (Roche #11814460001, 1:2000) and rabbit anti-α-tubulin antibodies (Abcam ab184970, 1:20,000). For Fig. 7B, Stain-Free technology (Bio-Rad) was used as a loading control.

Western blots were imaged with an Odyssey CLx system (LI-COR) using near-infrared fluorophore-labelled secondary antibodies. Signals were quantified (background correction: average) with Image Studio Version 3.1 (LI-COR). For quantification of vacuolar degradation of Fur4, three independent biological replicates with two technical replicates each were performed. Based on inspection of the blots, this number was deemed sufficient to account for variabilities in experimental conditions and detection of western blot signals. For each sample, the intensity of free GFP (800 nm channel) was normalised by division by the intensity of the tubulin loading control (700 nm channel). To account for variations in the amount of free GFP at t=0 in a given strain, these values were corrected by subtracting the normalised intensity at t=0. The resulting corrected signal of GFP at 4 h in the *bsd2Δ* strain was arbitrarily set to 1 for each individual western blot, and the other values were calculated relative to this reference point. For statistical analysis, unpaired two-tailed Student's *t*-tests were performed with GraphPad Prism 8.3.0, using all six values collected for each sample and time point.

Detection of Fur4 and Snc1 ubiquitylation

Fur4 ubiquitylation was detected by expression of Fur4^{myc} from a multicopy plasmid in the relevant yeast strains, preparation of a membrane-enriched lysate from exponential cultures as described previously (Galan et al., 1996) and SDS–PAGE followed by western blotting with an anti-myc antibody (9E10, produced in-house, 0.2 µg ml^{-1}). For detection of Snc1 ubiquitylation, relevant yeast strains expressing wild-type 3HA-tagged Snc1 (pRS416-3xHA-Snc1) or a mutant lacking lysine residues [pRS416-3xHA-Snc1(8KR)] were grown to exponential phase, treated – where indicated – with 2.4 mM H_2O_2 for 45 min at 30°C and subjected to total cell extraction with TCA (see above), followed by SDS–PAGE and western blot analysis using an anti-HA antibody (Santa Cruz sc-805, 1:5000).

Analysis of genetic interaction data

Genetic interaction profile similarities of relevant E2 and E3 genes (Table S1) and genetic interaction scores of *ubc13* and *mms2* (Table S2) were downloaded from http://www.thecellmap.org (Table S2) and used for histogram plots of correlation coefficients and interaction scores, respectively. GO term analysis of genetic interaction profile similarities was performed using goTermFinder (https://www.yeastgenome.org/goTermFinder), considering all genes with a score above 0.13 after removing duplicates.

Acknowledgements

We thank S. Braun, K. Schmidt and M. Berkenkopf for assistance with experiments, H.-P. Wollscheid and S. Wegmann for sharing biochemical expertise, and IMB's microscopy core facility and media laboratory for help and supplies. We are grateful to B. André, J. Azevedo, M. Ellison, M. Feldbrügge, J. Huibregtse, P. James, T. Graham, R. Klevit, D. Komander and T. Sommer for supplying reagents and advice.

Competing interests

The authors declare no competing or financial interests.

Author contributions

Conceptualization: C.R., H.D.U.; Methodology: C.R., V.A., V.T., T.K.A., O.S., S.C.J., S.L., H.D.U.; Formal analysis: A.K., H.D.U.; Investigation: C.R., V.A., V.T., T.K.A., O.S., S.C.J., H.D.U.; Data curation: A.K., H.D.U.; Writing - original draft: H.D.U.; Writing - review & editing: C.R., V.A., V.T., A.K., S.L., H.D.U.; Supervision: S.L., H.D.U.; Project administration: H.D.U.; Funding acquisition: H.D.U.

Funding

This work was funded by grants from the European Research Council to H.D.U. (ERC AdG 323179 and ERC PoC 786330).

Supplementary information

Supplementary information available online at
http://jcs.biologists.org/lookup/doi/10.1242/jcs.244566.supplemental

Peer review history

The peer review history is available online at
https://jcs.biologists.org/lookup/doi/10.1242/jcs.244566.reviewer-comments.pdf

References

Andersen, P. L., Zhou, H., Pastushok, L., Moraes, T., McKenna, S., Ziola, B., Ellison, M. J., Dixit, V. M. and Xiao, W. (2005). Distinct regulation of Ubc13 functions by the two ubiquitin-conjugating enzyme variants Mms2 and Uev1A. *J. Cell Biol.* **170**, 745-755. doi:10.1083/jcb.200502113

Araki, T. and Milbrandt, J. (2003). ZNRF proteins constitute a family of presynaptic E3 ubiquitin ligases. *J. Neurosci.* **23**, 9385-9394. doi:10.1523/JNEUROSCI.23-28-09385.2003

Araki, K., Kawamura, M., Suzuki, T., Matsuda, N., Kanbe, D., Ishii, K., Ichikawa, T., Kumanishi, T., Chiba, T., Tanaka, K. et al. (2003). A palmitoylated RING finger ubiquitin ligase and its homologue in the brain membranes. *J. Neurochem.* **86**, 749-762. doi:10.1046/j.1471-4159.2003.01875.x

Bagola, K., von Delbrück, M., Dittmar, G., Scheffner, M., Ziv, I., Glickman, M. H., Ciechanover, A. and Sommer, T. (2013). Ubiquitin binding by a CUE domain regulates ubiquitin chain formation by ERAD E3 ligases. *Mol. Cell* **50**, 528-539. doi:10.1016/j.molcel.2013.04.005

Bays, N. W., Gardner, R. G., Seelig, L. P., Joazeiro, C. A. and Hampton, R. Y. (2001). Hrd1p/Der3p is a membrane-anchored ubiquitin ligase required for ER-associated degradation. *Nat. Cell Biol.* **3**, 24-29. doi:10.1038/35050524

Bazirgan, O. A. and Hampton, R. Y. (2008). Cue1p is an activator of Ubc7p E2 activity in vitro and in vivo. *J. Biol. Chem.* **283**, 12797-12810. doi:10.1074/jbc.M801122200

Biederer, T., Volkwein, C. and Sommer, T. (1997). Role of Cue1p in ubiquitination and degradation at the ER surface. *Science* **278**, 1806-1809. doi:10.1126/science.278.5344.1806

Branigan, E., Plechanovová, A., Jaffray, E. G., Naismith, J. H. and Hay, R. T. (2015). Structural basis for the RING-catalyzed synthesis of K63-linked ubiquitin chains. *Nat. Struct. Mol. Biol.* **22**, 597-602. doi:10.1038/nsmb.3052

Burd, C. G. and Emr, S. D. (1998). Phosphatidylinositol(3)-phosphate signaling mediated by specific binding to RING FYVE domains. *Mol. Cell* **2**, 157-162. doi:10.1016/S1097-2765(00)80125-2

Carvalho, A. F., Pinto, M. P., Grou, C. P., Vitorino, R., Domingues, P., Yamao, F., Sá-Miranda, C. and Azevedo, J. E. (2012). High-yield expression in Escherichia coli and purification of mouse ubiquitin-activating enzyme E1. *Mol. Biotechnol.* **51**, 254-261. doi:10.1007/s12033-011-9463-x

Christensen, D. E. and Klevit, R. E. (2009). Dynamic interactions of proteins in complex networks: identifying the complete set of interacting E2s for functional investigation of E3-dependent protein ubiquitination. *FEBS J.* **276**, 5381-5389. doi:10.1111/j.1742-4658.2009.07249.x

Costanzo, M., Baryshnikova, A., Myers, C. L., Andrews, B. and Boone, C. (2011). Charting the genetic interaction map of a cell. *Curr. Opin. Biotechnol.* **22**, 66-74. doi:10.1016/j.copbio.2010.11.001

Costanzo, M., VanderSluis, B., Koch, E. N., Baryshnikova, A., Pons, C., Tan, G., Wang, W., Usaj, M., Hanchard, J., Lee, S. D. et al. (2016). A global genetic interaction network maps a wiring diagram of cellular function. *Science* **353**, aaf1420. doi:10.1126/science.aaf1420

Coumailleau, F., Das, V., Alcover, A., Raposo, G., Vandormael-Pournin, S., Le Bras, S., Baldacci, P., Dautry-Varsat, A., Babinet, C. and Cohen-Tannoudji, M. (2004). Over-expression of Rififylin, a new RING finger and FYVE-like domain-containing protein, inhibits recycling from the endocytic recycling compartment. *Mol. Biol. Cell* **15**, 4444-4456. doi:10.1091/mbc.e04-04-0274

Erpapazoglou, Z., Walker, O. and Haguenauer-Tsapis, R. (2014). Versatile roles of k63-linked ubiquitin chains in trafficking. *Cells* **3**, 1027-1088. doi:10.3390/cells3041027

Galan, J. M. and Haguenauer-Tsapis, R. (1997). Ubiquitin lys63 is involved in ubiquitination of a yeast plasma membrane protein. *EMBO J.* **16**, 5847-5854. doi:10.1093/emboj/16.19.5847

Galan, J. M., Moreau, V., Andre, B., Volland, C. and Haguenauer-Tsapis, R. (1996). Ubiquitination mediated by the Npi1p/Rsp5p ubiquitin-protein ligase is required for endocytosis of the yeast uracil permease. *J. Biol. Chem.* **271**, 10946-10952. doi:10.1074/jbc.271.18.10946

García-Rodríguez, N., Wong, R. P. and Ulrich, H. D. (2016). Functions of ubiquitin and SUMO in DNA replication and replication stress. *Front. Genet.* **7**, 87. doi:10.3389/fgene.2016.00087

Gietz, R. D. and Sugino, A. (1988). New yeast-*Escherichia coli* shuttle vectors constructed with in vitro mutagenized yeast genes lacking six-base pair restriction sites. *Gene* **74**, 527-534. doi:10.1016/0378-1119(88)90185-0

Hodge, C. D., Spyracopoulos, L. and Glove, J. N. M. (2016). Ubc13: the Lys63 ubiquitin chain building machine. *Oncotarget* **7**, 64471-64504. doi:10.18632/oncotarget.10948

Hoege, C., Pfander, B., Moldovan, G.-L., Pyrowolakis, G. and Jentsch, S. (2002). RAD6-dependent DNA repair is linked to modification of PCNA by ubiquitin and SUMO. *Nature* **419**, 135-141. doi:10.1038/nature00991

Hofmann, R. M. and Pickart, C. M. (1999). Noncanonical MMS2-encoded ubiquitin-conjugating enzyme functions in assembly of novel polyubiquitin chains for DNA repair. *Cell* **96**, 645-653. doi:10.1016/S0092-8674(00)80575-9

Husnjak, K. and Dikic, I. (2012). Ubiquitin-binding proteins: decoders of ubiquitin-mediated cellular functions. *Annu. Rev. Biochem.* **81**, 291-322. doi:10.1146/annurev-biochem-051810-094654

James, P., Halladay, J. and Craig, E. A. (1996). Genomic libraries and a host strain designed for highly efficient two-hybrid selection in yeast. *Genetics* **144**, 1425-1436.

Janke, C., Magiera, M. M., Rathfelder, N., Taxis, C., Reber, S., Maekawa, H., Moreno-Borchart, A., Doenges, G., Schwob, E., Schiebel, E. et al. (2004). A versatile toolbox for PCR-based tagging of yeast genes: new fluorescent proteins, more markers and promoter substitution cassettes. *Yeast* **21**, 947-962. doi:10.1002/yea.1142

Jin, H., Chiou, T.-T., Serwanski, D. R., Miralles, C. P., Pinal, N. and De Blas, A. L. (2014). Ring finger protein 34 (RNF34) interacts with and promotes γ-aminobutyric acid type-A receptor degradation via ubiquitination of the γ2 subunit. *J. Biol. Chem.* **289**, 29420-29436. doi:10.1074/jbc.M114.603068

Kampmeyer, C., Karakostova, A., Schenstrøm, S. M., Abildgaard, A. B., Lauridsen, A.-M., Jourdain, I. and Hartmann-Petersen, R. (2017). The exocyst subunit Sec3 is regulated by a protein quality control pathway. *J. Biol. Chem.* **292**, 15240-15253. doi:10.1074/jbc.M117.789867

Kim, H. T., Kim, K. P., Lledias, F., Kisselev, A. F., Scaglione, K. M., Skowyra, D., Gygi, S. P. and Goldberg, A. L. (2007). Certain pairs of ubiquitin-conjugating enzymes (E2s) and ubiquitin-protein ligases (E3s) synthesize nondegradable forked ubiquitin chains containing all possible isopeptide linkages. *J. Biol. Chem.* **282**, 17375-17386. doi:10.1074/jbc.M609659200

Komander, D. and Rape, M. (2012). The ubiquitin code. *Annu. Rev. Biochem.* **81**, 203-229. doi:10.1146/annurev-biochem-060310-170328

Kwon, Y. T. and Ciechanover, A. (2017). The ubiquitin code in the ubiquitin-proteasome system and autophagy. *Trends Biochem. Sci.* **42**, 873-886. doi:10.1016/j.tibs.2017.09.002

Li, M., Koshi, T. and Emr, S. D. (2015). Membrane-anchored ubiquitin ligase complex is required for the turnover of lysosomal membrane proteins. *J. Cell Biol.* **211**, 639-652. doi:10.1083/jcb.201505062

Liao, W., Xiao, Q., Tchikov, V., Fujita, K.-I., Yang, W., Wincovitch, S., Garfield, S., Conze, D., El-Deiry, W. S., Schütze, S. et al. (2008). CARP-2 is an endosome-associated ubiquitin ligase for RIP and regulates TNF-induced NF-κB activation. *Curr. Biol.* **18**, 641-649. doi:10.1016/j.cub.2008.04.017

Liao, W., Fujita, K.-I., Xiao, Q., Tchikov, V., Yang, W., Gunsor, M., Garfield, S., Goldsmith, P., El-Deiry, W. S., Schutze, S. et al. (2009). Response: CARP1 regulates induction of NF-κB by TNFα. *Curr. Biol.* **19**, R17-R19. doi:10.1016/j.cub.2008.11.041

Lorick, K. L., Jensen, J. P., Fang, S., Ong, A. M., Hatakeyama, S. and Weissman, A. M. (1999). RING fingers mediate ubiquitin-conjugating enzyme (E2)-dependent ubiquitination. *Proc. Natl Acad. Sci. USA* **96**, 11364-11369. doi:10.1073/pnas.96.20.11364

McCullough, J., Clague, M. J. and Urbé, S. (2004). AMSH is an endosome-associated ubiquitin isopeptidase. *J. Cell Biol.* **166**, 487-492. doi:10.1083/jcb.200401141

McDonald, E. R., III and El-Deiry, W. S. (2004). Suppression of caspase-8- and -10-associated RING proteins results in sensitization to death ligands and inhibition of tumor cell growth. *Proc. Natl Acad. Sci. USA* **101**, 6170-6175. doi:10.1073/pnas.0307459101

McKenna, S., Spyracopoulos, L., Moraes, T., Pastushok, L., Ptak, C., Xiao, W. and Ellison, M. J. (2001). Noncovalent interaction between ubiquitin and the human DNA repair protein Mms2 is required for Ubc13-mediated polyubiquitination. *J. Biol. Chem.* **276**, 40120-40126. doi:10.1074/jbc.M102858200

Metzger, M. B., Pruneda, J. N., Klevit, R. E. and Weissman, A. M. (2014). RING-type E3 ligases: master manipulators of E2 ubiquitin-conjugating enzymes and ubiquitination. *Biochim. Biophys. Acta* **1843**, 47-60. doi:10.1016/j.bbamcr.2013.05.026

Morawska, M. and Ulrich, H. D. (2013). An expanded tool kit for the auxin-inducible degron system in budding yeast. *Yeast* **30**, 341-351. doi:10.1002/yea.2967

Nikko, E. and Pelham, H. R. B. (2009). Arrestin-mediated endocytosis of yeast plasma membrane transporters. *Traffic* **10**, 1856-1867. doi:10.1111/j.1600-0854.2009.00990.x

Okiyoneda, T., Veit, G., Sakai, R., Aki, M., Fujihara, T., Higashi, M., Susuki-Miyata, S., Miyata, M., Fukuda, N., Yoshida, A. et al. (2018). Chaperone-independent peripheral quality control of CFTR by RFFL E3 ligase. *Dev. Cell* **44**, 694-708.e697. doi:10.1016/j.devcel.2018.02.001

Panier, S. and Durocher, D. (2009). Regulatory ubiquitylation in response to DNA double-strand breaks. *DNA Repair (Amst)* **8**, 436-443. doi:10.1016/j.dnarep.2009.01.013

Pickart, C. M. and Raasi, S. (2005). Controlled synthesis of polyubiquitin chains. *Methods Enzymol.* **399**, 21-36. doi:10.1016/S0076-6879(05)99002-2

Pohlmann, T., Baumann, S., Haag, C., Albrecht, M. and Feldbrügge, M. (2015). A FYVE zinc finger domain protein specifically links mRNA transport to endosome trafficking. *eLife* **4**, e06041. doi:10.7554/eLife.06041

Reggiori, F. and Pelham, H. R. B. (2002). A transmembrane ubiquitin ligase required to sort membrane proteins into multivesicular bodies. *Nat. Cell Biol.* **4**, 117-123. doi:10.1038/ncb743

Schindelin, J., Arganda-Carreras, I., Frise, E., Kaynig, V., Longair, M., Pietzsch, T., Preibisch, S., Rueden, C., Saalfeld, S., Schmid, B. et al. (2012). Fiji: an open-source platform for biological-image analysis. *Nat. Methods* **9**, 676-682. doi:10.1038/nmeth.2019

Shin, M. E., Ogburn, K. D., Varban, O. A., Gilbert, P. M. and Burd, C. G. (2001). FYVE domain targets Pib1p ubiquitin ligase to endosome and vacuolar membranes. *J. Biol. Chem.* **276**, 41388-41393. doi:10.1074/jbc.M105665200

Silva, G. M. and Vogel, C. (2015). Mass spectrometry analysis of K63-ubiquitinated targets in response to oxidative stress. *Data Brief* **4**, 130-134. doi:10.1016/j.dib.2015.05.002

Stenmark, H. and Aasland, R. (1999). FYVE-finger proteins–effectors of an inositol lipid. *J. Cell Sci.* **112**, 4175-4183.

Suryadinata, R., Roesley, S. N., Yang, G. and Šarčević, B. (2014). Mechanisms of generating polyubiquitin chains of different topology. *Cells* **3**, 674-689. doi:10.3390/cells3030674

Tibbetts, M. D., Shiozaki, E. N., Gu, L., McDonald, E. R., III, El-Deiry, W. S. and Shi, Y. (2004). Crystal structure of a FYVE-type zinc finger domain from the caspase regulator CARP2. *Structure* **12**, 2257-2263. doi:10.1016/j.str.2004.10.007

Ulrich, H. D. (2003). Protein-protein interactions within an E2-RING finger complex. Implications for ubiquitin-dependent DNA damage repair. *J. Biol. Chem.* **278**, 7051-7058. doi:10.1074/jbc.M212195200

Ulrich, H. D. and Jentsch, S. (2000). Two RING finger proteins mediate cooperation between ubiquitin-conjugating enzymes in DNA repair. *EMBO J.* **19**, 3388-3397. doi:10.1093/emboj/19.13.3388

Volland, C., Urban-Grimal, D., Geraud, G. and Haguenauer-Tsapis, R. (1994). Endocytosis and degradation of the yeast uracil permease under adverse conditions. *J. Biol. Chem.* **269**, 9833-9841.

Wei, P., Pan, D., Mao, C. and Wang, Y.-X. (2012). RNF34 is a cold-regulated E3 ubiquitin ligase for PGC-1α and modulates brown fat cell metabolism. *Mol. Cell. Biol.* **32**, 266-275. doi:10.1128/MCB.05674-11

Wood, V., Harris, M. A., McDowall, M. D., Rutherford, K., Vaughan, B. W., Staines, D. M., Aslett, M., Lock, A., Bahler, J., Kersey, P. J. et al. (2012). PomBase: a comprehensive online resource for fission yeast. *Nucleic Acids Res.* **40**, D695-D699. doi:10.1093/nar/gkr853

Wu, X. and Karin, M. (2015). Emerging roles of Lys63-linked polyubiquitylation in immune responses. *Immunol. Rev.* **266**, 161-174. doi:10.1111/imr.12310

Xu, P., Hankins, H. M., MacDonald, C., Erlinger, S. J., Frazier, M. N., Diab, N. S., Piper, R. C., Jackson, L. P., MacGurn, J. A. and Graham, T. R. (2017). COPI mediates recycling of an exocytic SNARE by recognition of a ubiquitin sorting signal. *eLife* **6**, e28342. doi:10.7554/eLife.28342

Yang, W., Rozan, L. M., McDonald, E. R., III, Navaraj, A., Liu, J. J., Matthew, E. M., Wang, W., Dicker, D. T. and El-Deiry, W. S. (2007). CARPs are ubiquitin ligases that promote MDM2-independent p53 and phospho-p53ser20 degradation. *J. Biol. Chem.* **282**, 3273-3281. doi:10.1074/jbc.M610793200

Zhang, R., Zhao, J., Song, Y., Wang, X., Wang, L., Xu, J., Song, C. and Liu, F. (2014). The E3 ligase RNF34 is a novel negative regulator of the NOD1 pathway. *Cell. Physiol. Biochem.* **33**, 1954-1962. doi:10.1159/000362972

Zheng, N. and Shabek, N. (2017). Ubiquitin ligases: structure, function, and regulation. *Annu. Rev. Biochem.* **86**, 129-157. doi:10.1146/annurev-biochem-060815-014922

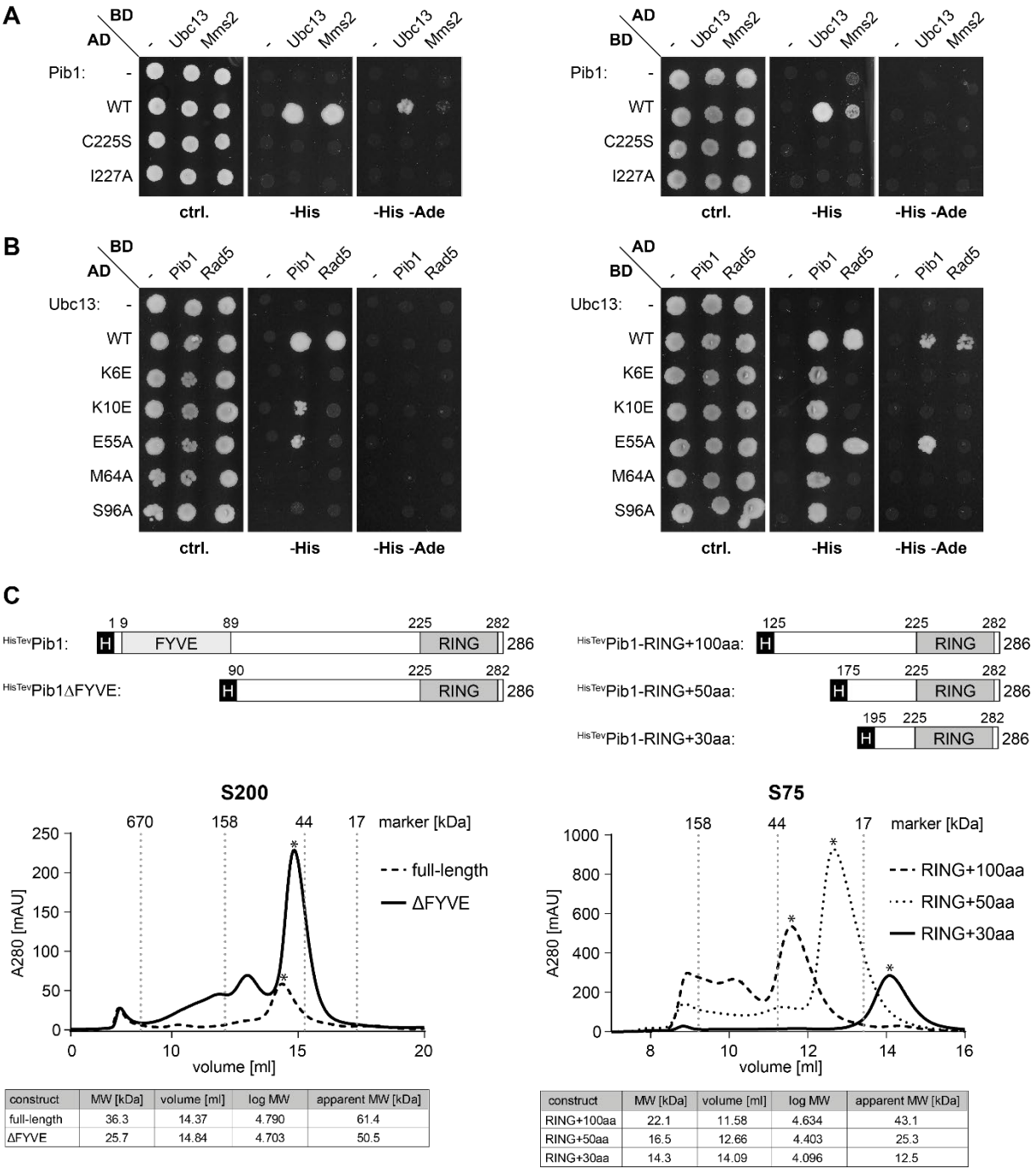

construct	MW [kDa]	volume [ml]	log MW	apparent MW [kDa]
full-length	36.3	14.37	4.790	61.4
ΔFYVE	25.7	14.84	4.703	50.5

construct	MW [kDa]	volume [ml]	log MW	apparent MW [kDa]
RING+100aa	22.1	11.58	4.634	43.1
RING+50aa	16.5	12.66	4.403	25.3
RING+30aa	14.3	14.09	4.096	12.5

Figure S1. Protein-protein interactions of Pib1, Ubc13 and Mms2.
(A) Mutations in the Pib1 RING domain abolish interactions with Ubc13 and Mms2 in the two-hybrid system. Assays were performed as described in Figure 1B.
(B) Mutations in Ubc13 that abolish interaction with Rad5 also affect interaction with Pib1. Two-hybrid assays were performed as described in Figure 1B.
(C) Pib1 dimerisation requires a domain N-terminal of its RING finger. Domain structures (numbering according to Pib1; H: His_6-Tev tag) and gel filtration profiles of the indicated recombinant His_6-TEV-tagged Pib1 constructs, expressed in *E. coli* and purified by Ni-NTA affinity chromatography. Profiles were recorded on calibrated (Gel Filtration Standard, BioRad) Superdex 200 or Superdex 75 10/300 GL columns. Asterisks indicate the relevant peaks. Tables beneath the elution profiles indicate elution volume and apparent as well as actual molecular weights.

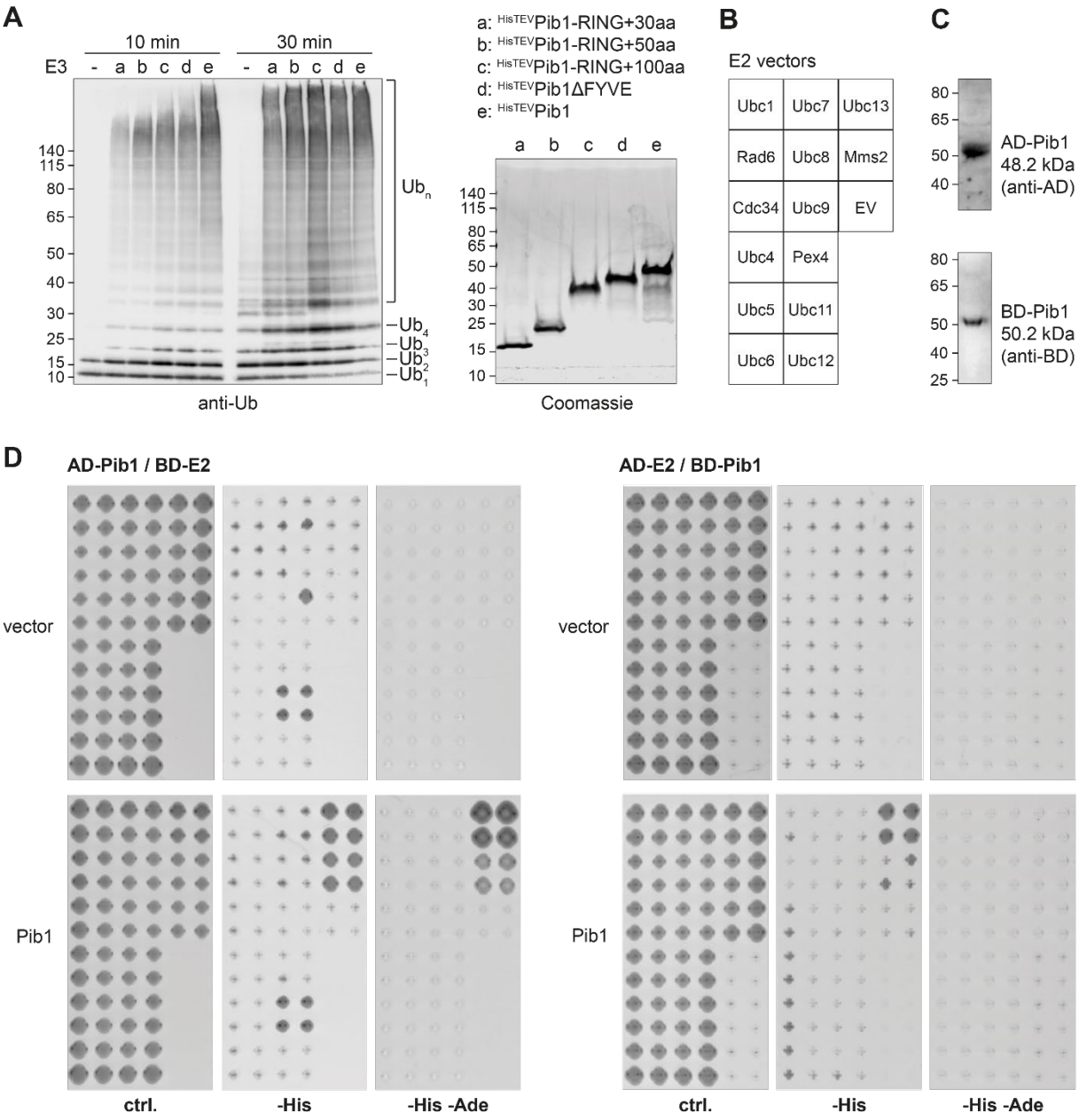

Figure S2. Pib1 is a cognate E3 for Ubc13-Mms2.

(A) Pib1 is most active as a dimer. *In vitro* polyubiquitin chain formation assays were carried out as described in Figure 2A, using the indicated His_6-TEV-tagged constructs. Reaction products are shown on the left (anti-ubiquitin blot); the right-hand panel shows a Coomassie-stained gel of the relevant E3 constructs.

(B-D) Among all budding yeast E2s, only Ubc13-Mms2 interacts with Pib1 in the two-hybrid system. Systematic two-hybrid interaction assays of Pib1 with all budding yeast E2s (and Mms2) were performed in diploid cells, generated by mating haploid a and α cells expressing the indicated Gal4 activation domain (AD) fusion constructs and Gal4 DNA-binding domain (BD) fusion constructs, respectively. Selected diploid cells were spotted as indicated in the scheme (EV: empty vector) **(B)**. Expression of Pib1 constructs was verified by western blotting of total cell extracts with anti-AD and anti-BD antibodies **(C)**, and cultures were subjected to growth analysis on selective plates **(D)**.

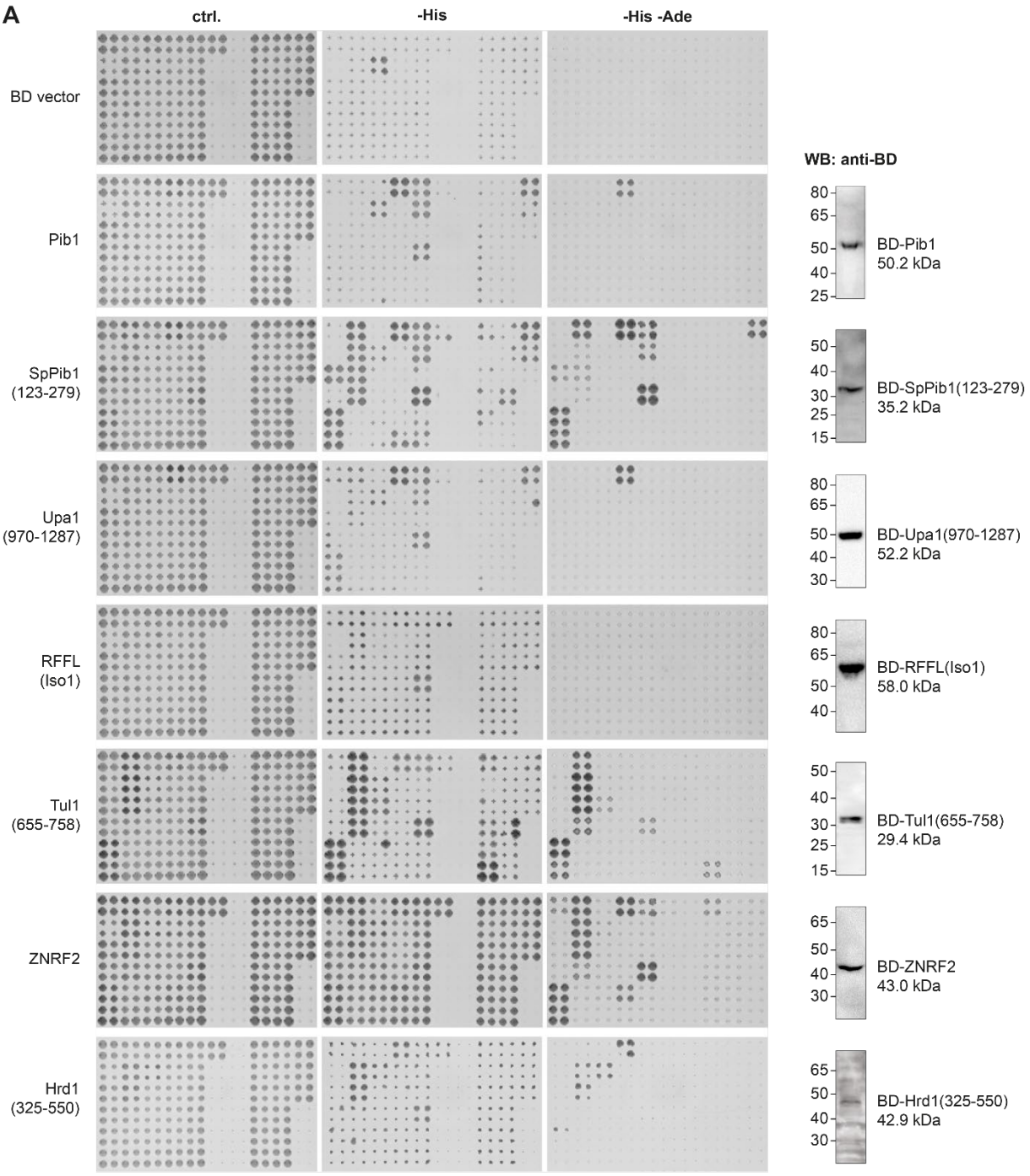

Figure S3. Interactions of selected membrane-associated E3s with E2s.
(A) Left: Systematic two-hybrid assays of relevant E3s with 30 human E2s and E2-like proteins and all budding yeast E2s, performed as described in Figure S2B-D. Right: images of the corresponding BD-E3 constructs, derived from western blots of total cell extracts using an anti-BD antibody. Note that the panels showing interactions of BD-Pib1 with yeast AD-E2s and the corresponding expression control are identical to those shown in Figures S2C and D, and are included here again for comparison.
(B) Spotting pattern of the human and budding yeast AD-E2 constructs for the systematic two-hybrid assays in (A) (EV: empty vector).

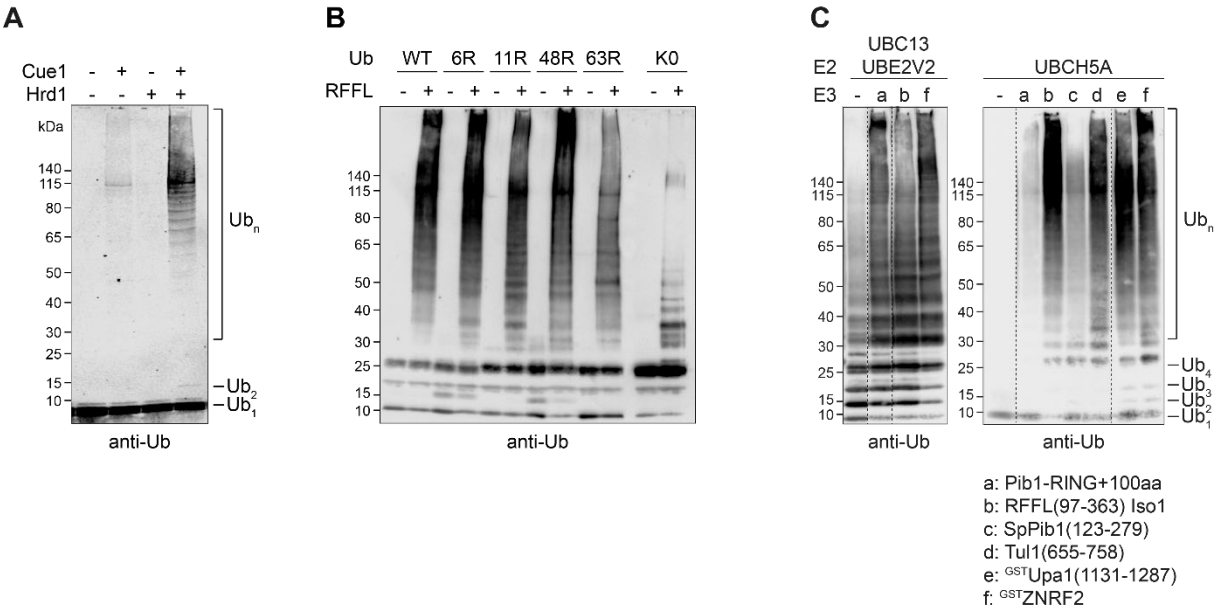

Figure S4. Activities of selected membrane-associated E3s with E2s.
(A) Hrd1 cooperates with Ubc7 in the presence of Cue1. Polyubiquitylation assays were performed as in Figure 3C-H, but with 100 μM ATP.
(B) RFFL-stimulated polyubiquitylation by Ubc4 results in heterogeneous linkages at multiple sites. Polyubiquitylation assays were performed as in Figure 3C-H with WT ubiquitin and indicated lysine mutants.
(C) Human E2s can substitute for yeast Ubc13-Mms2 and Ubc4. Left: Pib1 and human E3s stimulate polyubiquitin chain synthesis by human UBC13-UBE2V2. *In vitro* polyubiquitylation assays were performed as described in Figure 3C-G with the indicated E3 constructs, using UBC13-^{His}UBE2V2 as E2. Right: UBCH5A is activated by multiple E3s. *In vitro* polyubiquitylation assays were performed as described in Figure 3C-G with the indicated E3 constructs, using ^{His}UBCH5A as E2. Dashed lines indicate positions where irrelevant lanes were cut out of the image.

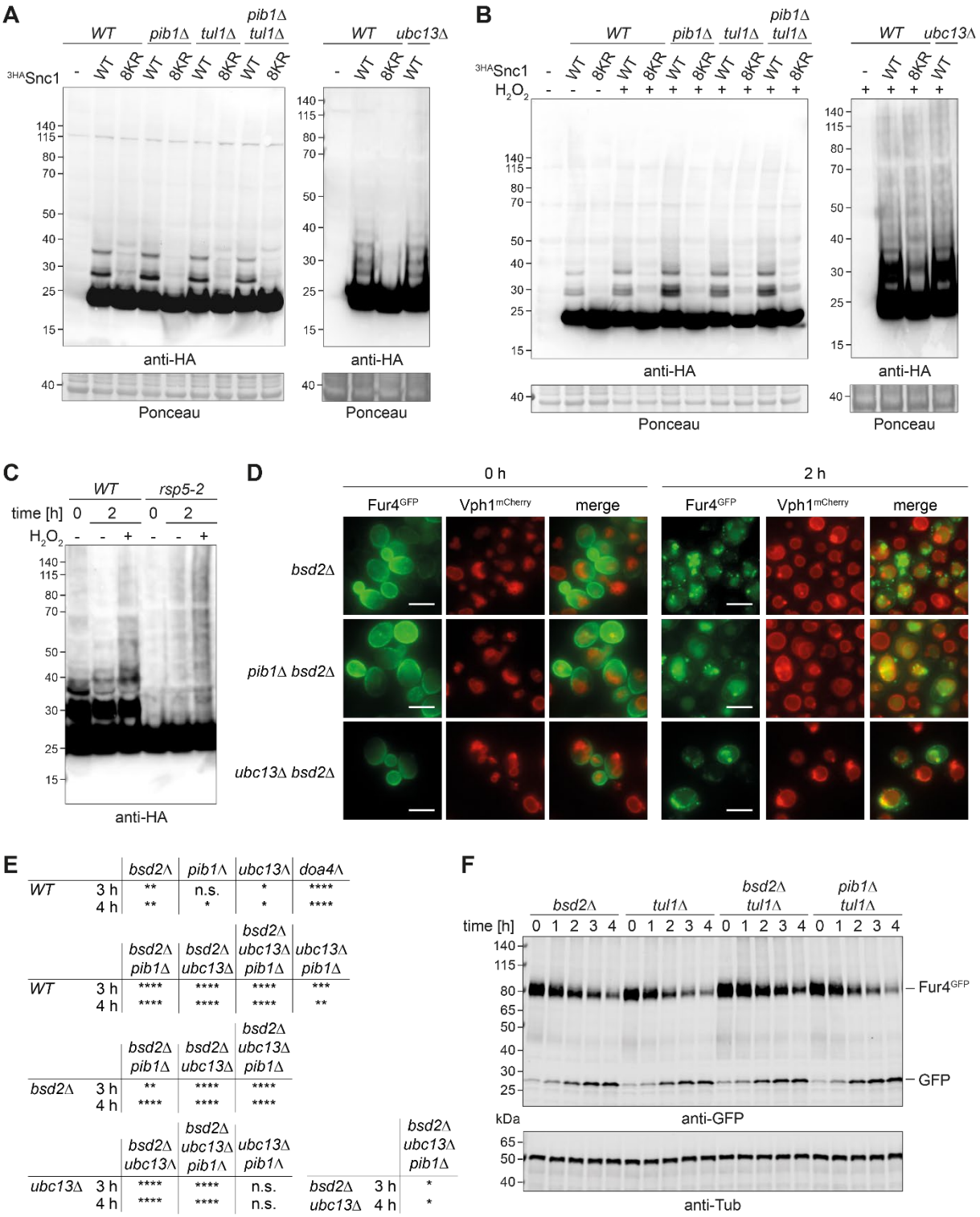

Figure S5. Pib1 contributes to membrane trafficking in a manner distinct from Tul1.

(A-B) Deletion of *PIB1* and/or *TUL1* does not impair overall ubiquitylation of Snc1. Ubiquitylation of ^{3HA}Snc1 (WT or a lysineless mutant, 8KR), expressed from a centromeric plasmid under control of the *TPI1* promoter, was analysed in the indicated strains by western blotting (anti-HA) of total cell extracts from exponentially growing cultures in the absence of H_2O_2 **(A)** or after incubation with 2.4 mM H_2O_2 at 30°C for 45 min **(B)**. Ponceau staining of the membrane served as loading control.

(C) Snc1 ubiquitylation is abolished in an *rsp5* mutant. ^{3HA}Snc1 modification was analysed as in (A-B).

(D) Deletion of *PIB1* or *UBC13* in a *bsd2Δ* background causes Fur4 accumulation in pre-vacuolar structures. Localization of Fur4^{GFP} and the vacuolar membrane protein Vph1^{mCherry} was analysed by fluorescence microscopy after induction of endocytosis as described in Figure 6C (scale bar = 5 µm).

(E) Statistical analysis of the data shown in Figure 6E. Two-tailed unpaired Student's t-tests were performed for the indicated data point pairs (3 h and 4 h) in order to obtain significance levels, using all values from three biological replicates with two technical replicates each (*: p<0.05; **: p<0.01; ***: p<0.001; ****: p<0.0001).

		bsd2Δ	pib1Δ	ubc13Δ	doa4Δ
WT	3 h	**	n.s.	*	****
	4 h	**	*	*	****

		bsd2Δ pib1Δ	bsd2Δ ubc13Δ	bsd2Δ ubc13Δ pib1Δ	ubc13Δ pib1Δ
WT	3 h	****	****	****	***
	4 h	****	****	****	**

		bsd2Δ pib1Δ	bsd2Δ ubc13Δ	bsd2Δ ubc13Δ pib1Δ
bsd2Δ	3 h	**	****	****
	4 h	****	****	****

		bsd2Δ ubc13Δ	bsd2Δ ubc13Δ pib1Δ	ubc13Δ pib1Δ
ubc13Δ	3 h	****	****	n.s.
	4 h	****	****	n.s.

		bsd2Δ ubc13Δ pib1Δ
bsd2Δ ubc13Δ	3 h	*
	4 h	*

(F) Tul1 does not contribute to vacuolar targeting of Fur4. Vacuolar delivery assays were performed in the indicated deletion strains as described in Figure 6D.

Table S1. Genetic interaction profile similarities of *UBC13*, *MMS2*, *UBC4*, *UBC5*, *UBC7*, *RAD6* and *PIB1*

source	thecellmap.org
downloaded	2019/01/10 (UBC13 and MMS2) and 2029/10/29 (UBC4, UBC5, UBC7, RAD6, PIB1)
content	genetic interaction profile similarities (**profile similarities**) for genes YDR092W (UBC13), YGL087C (MMS2), YBR082C (UBC4), YDR059C (UBC5), YMR022W (UBC7), YGL058W (RAD6) and YDR313C (PIB1)
description	Genes that share similar patterns of genetic interactions often belong to the same protein complex or biological pathway. The "profile similarities" spreadsheets consist of a ranked list of genes whose genetic interaction profiles most closely resemble the gene of interest. Genetic profile similarity is based on Pearson correlation.

Click here to Download Table S1

Table S2. Genetic interaction scores of *UBC13* and *MMS2*

source	thecellmap.org
downloaded	2019/01/10
content	genetic interactions scores (**GI Scores**) for genes YDR092W (UBC13) and YGL087C (MMS2)
description	The genetic interaction score (ε) measures the extent to which a double mutant colony size deviates from the colony size expected from combining two mutations together. Negative genetic interaction scores indicate putative synthetic sick/lethal interactions whereas positive genetic interaction scores indicate potential epistatic or suppression interactions involving the genes of interest. The magnitude of the genetic interaction score is indicative of the strength of interaction. According to Costanzo et al. (Science 2016, 353:aaf1420), the intermediate cutoff for significant genetic interactions consists of a combination of p-value < 0.05 and $\|\varepsilon\| > 0.08$. More stringent thresholds on negative interactions (p-value < 0.05 and $\varepsilon < -0.12$) and positive interactions (p-value < 0.05 and $\varepsilon > 0.16$) can be considered.

Click here to Download Table S2

Table S3. Yeast strains used in this study

Strain	ID	Relevant Genotype	Source/ Reference
PJ69-4A	195	*MAT**a** trp1-901 leu2-3,112 ura3-52 his3-200, gal4Δ gal80Δ LYS2::GAL1-HIS3 GAL2-ADE2 met2::GAL7-lacZ*	(1)
PJ69-4α	196	*MAT**α** trp1-901 leu2-3,112 ura3-52 his3-200, gal4Δ gal80Δ LYS2::GAL1-HIS3 GAL2-ADE2 met2::GAL7-lacZ*	(1)
Y2H *mms2Δ*	n.a.	PJ69-4A *mms2::kanMX*	This study
Y2H *ubc13Δ*	n.a.	PJ69-4A *ubc13::kanMX*	This study
BY4741 (*WT*)	790	*MAT**a** his3Δ1 leu2Δ0 met15Δ0 ura3Δ0*	Euroscarf
bsd2Δ	n.a.	*BY4741 bsd2::kanMX*	Dharmacon
doa4Δ	4474	*BY4741 doa4::kanMX*	Dharmacon
pib1Δ	840	*BY4741 pib1::kanMX*	Dharmacon
ubc13Δ	791	*BY4741 ubc13::kanMX*	Dharmacon
npi1	n.a.	*BY4741 rsp5::kanMX* (*kanMX* insertion in the promoter)	(2)
bsd2Δ pib1Δ	4992	*BY4741 bsd2::kanMX pib1::his3MX*	This study
bsd2Δ ubc13Δ	2905	*BY MAT**a** his3Δ1 leu2Δ0 ura3Δ0 [met15Δ0 and lys2Δ0 not scored] bsd2::kanMX ubc13::kanMX*	This study
bsd2Δ mms2Δ	n.a.	*BY4741 bsd2:::hphNT1 mms2::kanMX*	This study
bsd2Δ pib1Δ ubc13Δ	4993	*BY MAT**a** his3Δ1 leu2Δ0 ura3Δ0 [met15Δ0 and lys2Δ0 not scored] bsd2::kanMX pib1::his3MX ubc13::kanMX*	This study
pib1Δ ubc13Δ	2906	*BY MAT**α** his3Δ1 leu2Δ0 ura3Δ0 [met15Δ0 and lys2Δ0 not scored] pib1::kanMX ubc13::kanMX*	This study
tul1Δ	4282	*BY4741 tul1::hphNT1*	This study
bsd2Δ tul1Δ	4284	*BY4741 bsd2::kanMX tul1::hphNT1*	This study
pib1Δ tul1Δ	4283	*BY4741 pib1::kanMX tul1::hphNT1*	This study
$PIB1^{mCherry}$	4994	*BY4741* $PIB1^{mCherry}$*::his3MX*	This study
$PIB1^{mCherry}$ $UBC13^{GFP}$	4995	*BY4741* $PIB1^{mCherry}$*::his3MX* $UBC13^{yeGFP}$*::natNT2*	This study
$UBC13^{GFP}$ *pib1Δ*	4996	*BY4741* $UBC13^{yeGFP}$*::natNT2 pib1::his3MX*	This study
$UBC13^{GFP}$ *pib1Δ mms2Δ*	4997	*BY4741* $UBC13^{yeGFP}$*::natNT2 pib1::his3MX mms2::hphNT1*	This study
$MMS2^{GFP}$ *pib1Δ*	4998	*BY4741* $MMS2^{yeGFP}$*::natNT2 pib1::his3MX*	This study
$MMS2^{GFP}$ *pib1Δ ubc13Δ*	4999	*BY MAT**α** his3Δ1 leu2Δ0 ura3Δ0 [met15Δ0 and lys2Δ0 not scored]* $MMS2^{yeGFP}$*::natNT2 pib1::kanMX ubc13::kanMX*	This study
$VPH1^{mCherry}$ *bsd2Δ*	n.a.	*BY4741* $VPH1^{mCherry}$*::natNT2 bsd2::kanMX*	This study
$VPH1^{mCherry}$ *bsd2Δ pib1Δ*	n.a.	*BY4741* $VPH1^{mCherry}$*::natNT2 bsd2::hphNT1 pib1::kanMX*	This study
$VPH1^{mCherry}$ *bsd2Δ ubc13Δ*	n.a.	*BY4741* $VPH1^{mCherry}$*::natNT2 bsd2::hphNT1 ubc13::kanMX*	This study
DF5	003	*his3-Δ200 leu2-3,2-112 lys2-801 trp1-1(am) ura3-52*	(3)
DF5 mms2Δ	029	*DF5 mms2::HIS3*	(4)

DF5 ubc13Δ	345	*DF5 ubc13::HIS3*	(4)
DF5 rsp5-2	592	*DF5 rsp5-2*	(5)
SUB280	412	*DF5 ubi1-Δ1::TRP1 ubi2-Δ2::URA3 ubi3-Δub-2 ubi4-Δ2::LEU2 [pUB39 pUB100]*	(6)
SUB280 ubc13Δ	426	*SUB280 ubc13::kanMX*	This study
SUB280 pib1Δ	463	*SUB280 pib1::kanMX*	This study
SUB413 [ubi(K63R)]	464	*DF5 ubi1-Δ1::TRP1 ubi2-Δ2::URA3 ubi3-Δub-2 ubi4-Δ2::LEU2 [pUB39(K63R) pUB100]*	(6)

References:

(1) James P, Halladay J, Craig EA (1996) Genomic libraries and a host strain designed for highly efficient two-hybrid selection in yeast. *Genetics* **144:** 1425-1436

(2) Léon S, Erpapazoglou Z, Haguenauer-Tsapis R (2008) Ear1p and Ssh4p are new adaptors of the ubiquitin ligase Rsp5p for cargo ubiquitylation and sorting at multivesicular bodies. *Mol Biol Cell* **19**: 2379-2388

(3) Finley D, Ozkaynak E, Varshavsky A (1987) The yeast polyubiquitin gene is essential for resistance to high temperatures, starvation, and other stresses. *Cell* **48**: 1035-1046

(4) Ulrich HD, Jentsch S (2000) Two RING finger proteins mediate cooperation between ubiquitin-conjugating enzymes in DNA repair. *EMBO J* **19**: 3388-3397

(5) Hoppe T, Matuschewski K, Rape M, Schlenker S, Ulrich HD, Jentsch S (2000) Activation of a membrane-bound transcription factor by regulated ubiquitin/proteasome-dependent processing. *Cell* **102**: 577-586

(6) Spence J, Sadis S, Haas AL, Finley D (1995) A ubiquitin mutant with specific defects in DNA repair and multiubiquitination. *Mol Cell Biol* **15**: 1265-1273

Table S4. Plasmids used in this study

Name	ID	Use	Source/Reference
pGAD-C1	pHU191	Y2H assays	(1)
pGBD-C1	pHU194	Y2H assays	(1)
pGAD-Ubc13	pHU281	Y2H assays	(2)
pGBD-Ubc13	pHU282	Y2H assays	(2)
pGAD-Ubc13 w/o intron	pHU2812	Y2H assays (E2 screen)	This study
pGBD-Ubc13 w/o intron	pHU2813	Y2H assays (E2 screen)	This study
pGAD-Ubc13(K6E)	pHU511	Y2H assays	(3)
pGBD-Ubc13(K6E)	pHU512	Y2H assays	(3)
pGAD-Ubc13(K10E)	pHU513	Y2H assays	(3)
pGBD-Ubc13(K10E)	pHU514	Y2H assays	(3)
pGAD-Ubc13(E55A)	pHU592	Y2H assays	(3)
pGBD-Ubc13(E55A)	pHU589	Y2H assays	(3)
pGAD-Ubc13(M64A)	pHU594	Y2H assays	(3)
pGBD-Ubc13(M64A)	pHU590	Y2H assays	(3)
pGAD-Ubc13(S96A)	pHU593	Y2H assays	(3)
pGBD-Ubc13(S96A)	pHU591	Y2H assays	(3)
pGAD-Mms2	pHU098	Y2H assays (general & E2 screen)	(2)
pGBD-Mms2	pHU099	Y2H assays (general & E2 screen)	(2)
pGBDU-Mms2	pHU200	Y2H assays (genomic screen)	This study
pGBD-Ubc1	pHU279	Y2H assays (E2 screen)	This study
pGAD-Ubc1	pHU500	Y2H assays (E2 screen)	This study
pGAD-Rad6	pHU103	Y2H assays (E2 screen)	(2)
pGBD-Rad6	pHU102	Y2H assays (E2 screen)	(2)
pGAD-Cdc34	pHU515	Y2H assays (E2 screen)	This study
pGBD-Cdc34	pHU516	Y2H assays (E2 screen)	This study
pGAD-Ubc4	pHU271	Y2H assays (E2 screen)	This study
pGBD-Ubc4	pHU272	Y2H assays (E2 screen)	This study
pGAD-Ubc5	pHU1469	Y2H assays (E2 screen)	This study
pGBD-Ubc5	pHU1470	Y2H assays (E2 screen)	This study
pGAD-Ubc6	pHU1471	Y2H assays (E2 screen)	This study
pGBD-Ubc6	pHU1472	Y2H assays (E2 screen)	This study
pGAD-Ubc7	pHU1473	Y2H assays (E2 screen)	This study
pGBD-Ubc7	pHU1474	Y2H assays (E2 screen)	This study
pGAD-Ubc8	pHU269	Y2H assays (E2 screen)	This study
pGBD-Ubc8	pHU270	Y2H assays (E2 screen)	This study
pGAD-Ubc9	pHU273	Y2H assays (E2 screen)	This study
pGBD-Ubc9	pHU274	Y2H assays (E2 screen)	This study
pGAD-Pex4	pHU517	Y2H assays (E2 screen)	This study
pGBD-Pex4	pHU518	Y2H assays (E2 screen)	This study
pGAD-Ubc11	pHU519	Y2H assays (E2 screen)	This study
pGBD-Ubc11	pHU520	Y2H assays (E2 screen)	This study
pGAD-Ubc12	pHU3141	Y2H assays (E2 screen)	This study
pGBD-Ubc12	pHU3142	Y2H assays (E2 screen)	This study

pGAD-Pib1	pHU222	Y2H assays	This study
pGBD-Pib1	pHU280	Y2H assays	This study
pGAD-C1-Pib1	pHU2808	Y2H assays (E2 screen)	This study
pGBD-C1-Pib1	pHU2809	Y2H assays (E2 screen)	This study
pGAD-Pib1(C225S)	pHU524	Y2H assays	This study
pGBD-Pib1(C225S)	pHU525	Y2H assays	This study
pGBD-Pib1(I227A)	pHU741	Y2H assays	This study
pGAD-Pib1(I227A)	pHU798	Y2H assays	This study
pGAD-Rad5	pHU188	Y2H assays	(2)
pGBD-Rad5	pHU189	Y2H assays	(2)
pGBD-RFFL(Iso1)	pHU3134	Y2H assays (E2 screen)	This study
pGBD-Upa1(970-1287)	pHU3138	Y2H assays (E2 screen)	This study
pGBD-SpPib1(123-279)	pHU3202	Y2H assays (E2 screen)	This study
pGBD-ZNRF2	pHU3212	Y2H assays (E2 screen)	This study
pGBD-Tul1(655-758)	pHU3743	Y2H assays (E2 screen)	This study
pGBD-Hrd1(325-551)	pHU4370	Y2H assays (E2 screen)	This study
pGEX-4T-1	pHU243	Protein purification	GE Healthcare
pTER32 pET3a-Ub(K0)	pHU679	Protein purification	Michael J. Ellison*
pTER88 pET3a-Ub(K48R)	pHU682	Protein purification	Michael J. Ellison*
pET3a-Ub(K63R)	pHU684	Protein purification	(4)
pET3a-Ub(K11R)	pHU3599	Protein purification	This study
pET28-His_6-mE1	pHU2448	Protein purification	(5, Addgene #32534)
pET21(+)-His_6-Ubc13	pHU3010	Protein purification	This study
pHISTEV30a-hUBC13	pHU3760	Protein purification	(6)
pGEX-6P-1-Ubc13(K92R)	pHU3443	Protein purification	This study
pET21(+)-His_6-Mms2	pHU3009	Protein purification	This study
pET30-His_6-TEV-Mms2	pHU2807	Protein purification	This study
pET21(+)-His_6-UBE2V2	pHU3606	Protein purification	This study
pQE32-His_6-VSV-Rad6	pHU116	Protein purification	This study
pET16b-His_6-Cdc34	pHU808	Protein purification	Michael J. Ellison*
pET21(+)-His_6-Ubc4	pHU3472	Protein purification	This study
pGEX-6P-1-Ubc4(K91R)	pHU3592	Protein purification	This study
pQE30-His_6-Ubc5	pHU1468	Protein purification	This study
pET22b-His_6-UBCH5A	pHU3351	Protein purification	This study
pMAL-TEV2-Ubc7-His_6	pHU3365	Protein purification	This study
pMAL-TEV-His_6-Ubc7	pHU3451	Protein purification	This study
pGEX-6P-1-Pib1ΔFYVE	pHU2578	Protein purification	This study
pET30-His_6-TEV-Pib1RING+30aa	pHU3017	Protein purification	This study
pET30-His_6-TEV-Pib1RING+50aa	pHU3018	Protein purification	This study
pET30-His_6-TEV-Pib1RING+100aa	pHU3019	Protein purification	This study
pET30-His_6-TEV-Pib1ΔFYVE	pHU3020	Protein purification	This study
pET30-His_6-TEV-Pib1	pHU3021	Protein purification	This study
pGEX-6P-Cue1-His_6	pHU2458	Protein purification	(7)
pGEX-6P-HA-Rsp5	pHU3473	Protein purification	(8)
pGEX-6P-1-RFFL(97-363) Iso1	pHU3016	Protein purification	This study

pGEX-6P-1-Upa1(1131-1287)	pHU3025	Protein purification	This study
pGEX-6P-1-SpPib1(123-279)	pHU3204	Protein purification	This study
pGEX-2TK-ZNRF2	pHU3213	Protein purification	This study
pGEX-6P-1-Tul1(655-758)	pHU3741	Protein purification	This study
pGEX-Hrd1(325-551)	pHU2459	Protein purification	(7)
pGEX-6P-1-AMSH	pHU2898	Protein purification	(9)
YCp33-CUP1-RFFL(Iso1)-yeGFP	pHU3055	Microscopy	This study
YCp33-CUP1-Upa1(970-1287)-yeGFP	pHU3057	Microscopy	This study
YCp33-CUP1-SpPib1-yeGFP	pHU3434	Microscopy	This study
YCp33-CUP1-Pib1-mCherry	pHU4030	Microscopy	This study
YCp33-CUP1-Pib1(I227A)-mCherry	pHU4344	Microscopy	This study
YCp33-CUP1-Hrd1-mCherry	pHU4386	Microscopy	This study
pFA6a-his3MX6	pHU233	Template for PCR deletion	(10)
pFA6a-hphNT1	pHU1634	Template for PCR deletion	(11, Euroscarf P30347)
pFA6a-kanMX6	pHU452	Template for PCR deletion	(12, Addgene #39296)
pYM-yeGFP-natNT2	pHU2442	Template for PCR tagging	This study
pYM-mCherry-his3MX6	pHU2586	Template for PCR tagging	This study
YCplac33-GAL-Fur4-yeGFP	pHU2581	endocytosis assays	This study
YEplac195-Fur4-myc	pHU0304	endocytosis assays	This study
pRS416-ADH-GFP-Smf1	pSL31	endocytosis assays	(13)
pRS416-3HA-Snc1	pHU3748	Snc1 ubiquitylation assays	(14)
pRS416-3HA-Snc1(8KR)	pHU3748	Snc1 ubiquitylation assays	(14)

* Michael J. Ellison (University of Alberta, Department of Biochemistry, 474 Medical Sciences Building, Edmonton, Alberta, Canada T6G 2R3)

References:

(1) James P, Halladay J, Craig EA (1996) Genomic libraries and a host strain designed for highly efficient two-hybrid selection in yeast. *Genetics* **144:** 1425-1436

(2) Ulrich HD, Jentsch S (2000) Two RING finger proteins mediate cooperation between ubiquitin-conjugating enzymes in DNA repair. *EMBO J* **19:** 3388-3397

(3) Ulrich HD (2003) Protein-protein interactions within an E2-RING finger complex. Implications for ubiquitin-dependent DNA damage repair. *J Biol Chem* **278:** 7051-7058

(4) Parker JL, Ulrich HD (2009) Mechanistic analysis of PCNA poly-ubiquitylation by the ubiquitin protein ligases Rad18 and Rad5. *EMBO J* **28:** 3657-3666

(5) Carvalho AF, Pinto MP, Grou CP, Vitorino R, Domingues P, Yamao F, Sa-Miranda C, Azevedo JE (2012) High-yield expression in *Escherichia coli* and purification of mouse ubiquitin-activating enzyme E1. *Mol Biotechnol* **51:** 254-261

(6) Branigan E, Plechanovova A, Jaffray EG, Naismith JH, Hay RT (2015) Structural basis for the RING-catalyzed synthesis of K63-linked ubiquitin chains. *Nat Struct Mol Biol* **22:** 597-602

(7) Bagola K, von Delbruck M, Dittmar G, Scheffner M, Ziv I, Glickman MH, Ciechanover A, Sommer T (2013) Ubiquitin binding by a CUE domain regulates ubiquitin chain formation by ERAD E3 ligases. *Mol Cell* **50:** 528-539

(8) Wang G, Yang J, Huibregtse JM (1999) Functional domains of the Rsp5 ubiquitin-protein ligase. *Mol Cell Biol* **19:** 342-352

(9) Hospenthal MK, Mevissen TET, Komander D (2015) Deubiquitinase-based analysis of ubiquitin chain architecture using Ubiquitin Chain Restriction (UbiCRest). *Nat Protoc* **10:** 349-361

(10) Longtine MS, McKenzie A 3rd, Demarini DJ, Shah NG, Wach A, Brachat A, Philippsen P, Pringle JR (1998) Additional modules for versatile and economical PCR-based gene deletion and modification in *Saccharomyces cerevisiae*. *Yeast* **14**: 953-61

(11) Janke C, Magiera MM, Rathfelder N, Taxis C, Reber S, Maekawa H, Moreno-Borchart A, Doenges G, Schwob E, Schiebel E, Knop M (2004) A versatile toolbox for PCR-based tagging of yeast genes: new fluorescent proteins, more markers and promoter substitution cassettes. *Yeast* **21:** 947-962

(12) Bahler J, Wu JQ, Longtine MS, Shah NG, McKenzie A 3rd, Steever AB, Wach A, Philippsen P, Pringle JR (1998) Heterologous modules for efficient and versatile PCR-based gene targeting in *Schizosaccharomyces pombe*. *Yeast* **14**: 943-951

(13) Léon S, Erpapazoglou Z, Haguenauer-Tsapis R (2008) Ear1p and Ssh4p are new adaptors of the ubiquitin ligase Rsp5p for cargo ubiquitylation and sorting at multivesicular bodies. *Mol Biol Cell* **19**: 2379-2388

(14) Xu P, Hankins HM, MacDonald C, Erlinger SJ, Frazier MN, Diab NS, Piper RC, Jackson LP, MacGurn JA, Graham TR (2017) COPI mediates recycling of an exocytic SNARE by recognition of a ubiquitin sorting signal. *Elife* **6:** 10.7554/eLife.28342

Table S5. Protein purifications

Protein	Plasmid	Expression	Reference/Purification	Figure
GST	pGEX-4T-1 (pHU243)	BL21 CodonPlus (DE3) RIL 1 mM IPTG, 37°C, 4 h	GSH-Sepharose: batch	1D 2D
^{GST}AMSH	pGEX-6P-1-AMSH (pHU2898)	BL21 CodonPlus (DE3) RIL 1 mM IPTG, 20°C, o.n.	(1) GSH-Sepharose: batch	2C
^{His}Uba1	pET28-His6-mE1 (pHU2448)	BL21 (DE3) 0.5 mM IPTG, 16°C, o.n.	(2)	all reactions
Ub(K0)	pET3a-Ub(K0) (pHU679)	BL21 pLysS 1 mM IPTG, 37°C, 4 h	(3) 1. Lysis at pH 4.0 2. Heat: 70 °C 3. Resource S 4. Superdex 75	S4B
Ub(K11R)	pET3a-Ub(K11R) (pHU3599)	BL21 pLysS 1 mM IPTG, 37°C, 4 h	(3) 1. Lysis at pH 4.0 2. Heat: 70 °C 3. Resource S 4. Superdex 75	S4B
Ub(K48R)	pET3a-Ub(K48R) (pHU682)	BL21 pLysS 1 mM IPTG, 18°C, o.n.	(3) 1. Lysis at pH 4.0 2. Heat: 70 °C 3. Resource S 4. Superdex 75	2G S4B
Ub(K63R)	pET3a-Ub(K63R) (pHU684)	BL21 pLysS 1 mM IPTG, 18°C, o.n.	(3) 1. Lysis at pH 4.0 2. Heat: 70 °C 3. Resource S 4. Superdex 75	2B,E,F 3C-H S4B
E2s				
^{His}Ubc13	pET21(+)-His$_6$-Ubc13 (pHU3010)	BL21 CodonPlus (DE3) RIL 1 mM IPTG, 20°C, o.n.	1. IMAC: batch 2. Superdex 75	1D 2A-G 3C-H S2A S4A
Ubc13(K92R)	pGEX-6P-1- Ubc13(K92R) (pHU3443)	BL21 CodonPlus (DE3) RIL 1 mM IPTG, 18°C, o.n.	1. GSH-Sepharose: batch 2. Pre-Scission cleavage 3. GSTrap HP 5 ml: 2 runs 4. Superdex 75	2H
human UBC13	pHISTEV30a-hUBC13 (pHU3760)	BL21 CodonPlus (DE3) RIL 1 mM IPTG, 18°C, o.n.	(4) 1. IMAC: batch 2. TEV cleavage 3. IMAC: batch 4. Superdex 75	S4C
^{His}Mms2	pET21(+)-His$_6$-Mms2 (pHU3009)	BL21 CodonPlus (DE3) RIL 1 mM IPTG, 20°C, o.n.	1. IMAC: batch 2. Superdex 75	1D 2D
Mms2	pET30-His$_6$-TEV-Mms2 (pHU2807)	BL21 CodonPlus (DE3) RIL 0.1 mM IPTG, 20°C, o.n.	1. IMAC: batch 2. TEV cleavage 3. IMAC: batch 4. Superdex 75	2A-C,E-H 3C-H S2A S4A
^{His}UBE2V2	pET21(+)-His$_6$-UBE2V2 (pHU3606)	BL21 CodonPlus (DE3) RIL 1 mM IPTG, 18°C, o.n.	1. IMAC: batch 2. Superdex 75	S4C
^{His}Rad6	pQE32-His$_6$-VSV-Rad6 (pHU116)	BL21 CodonPlus (DE3) RIL 1 mM IPTG, 20°C, o.n.	IMAC: batch	2D
^{His}Cdc34	pET16b-His$_6$-Cdc34 (pHU808)	BL21 CodonPlus (DE3) RIL 1 mM IPTG, 20°C, o.n.	IMAC: batch	2D

^{His}Ubc4	pET21(+)-His$_6$-Ubc4 (pHU3472)	BL21 CodonPlus (DE3) RIL 1 mM IPTG, 18°C, o.n.	1. IMAC: batch 2. Superdex 75	2D-G 3C-H S4A, B
Ubc4(K91R)	pGEX-6P-1-Ubc4(K91R) (pHU3592)	BL21 CodonPlus (DE3) RIL 1 mM IPTG, 18°C, o.n.	1. GSH-Sepharose: batch 2. PreScission cleavage 3. GSTrap HP 5 ml: 2 runs 4. Superdex 75	2I
^{His}Ubc5	pQE30-His$_6$-Ubc5 (pHU1468)	BL21 CodonPlus (DE3) RIL 1 mM IPTG, 20°C, o.n.	IMAC: batch	2D
^{His}Ubc7	pMAL-TEV-His$_6$-Ubc7 (pHU3451)	BL21 CodonPlus (DE3) RIL 0.5 mM IPTG, 18°C, 6 h	1. IMAC: batch 2. TEV cleavage 3. IMAC: batch 4. HiTrap Q SP 5ml, pH 7.5 5. Superdex 75	2D
Ubc7^{His}	pMAL-TEV2-Ubc7-His$_6$ (pHU3365)	BL21 CodonPlus (DE3) RIL 0.5 mM IPTG, 18°C, 6 h	1. IMAC: batch 2. TEV cleavage 3. IMAC: batch 4. HiTrap Q SP 5ml, pH 7.5 5. Superdex 75	2E-G 3C-H S4A
^{His}UBCH5A	pET22b-His$_6$-UBCH5A (pHU3351)	BL21 CodonPlus (DE3) RIL 0.2 mM IPTG, 37°C, 5 h	IMAC: batch	S4C
E3s				
^{GST}Pib1ΔFYVE	pGEX-6P-1-Pib1ΔFYVE (aa 91-286) (pHU2578)	BL21 CodonPlus (DE3) RIL 1 mM IPTG, 18°C, o.n. 50 µM $ZnCl_2$	1. GSH-Sepharose: batch 2. Superdex 200	1D 2A-E
^{HisTEV}Pib1	pET30-His$_6$-TEV-Pib1 (pHU3021)	BL21 CodonPlus (DE3) RIL 1 mM IPTG, 20°C, o.n. 50 µM $ZnCl_2$	1. IMAC: batch 2. Superdex 200	S1C S2A
^{HisTEV}Pib1ΔFYVE	pET30-His$_6$-TEV-Pib1ΔFYVE (aa 91-286) (pHU3020)	BL21 CodonPlus (DE3) RIL 1 mM IPTG, 20°C, o.n. 50 µM $ZnCl_2$	1. IMAC: batch 2. Superdex 200	S1C S2A
^{HisTEV}Pib1RING +100aa	pET30-His$_6$-TEV-Pib1RING+100aa (aa 125-286) (pHU3019)	BL21 CodonPlus (DE3) RIL 1 mM IPTG, 20°C, o.n. 50 µM $ZnCl_2$	1. IMAC: batch 2. Superdex S75	S1C S2A
Pib1RING +100aa	pET30-His$_6$-TEV-Pib1RING+100aa (aa 125-286) (pHU3019)	BL21 CodonPlus (DE3) RIL 1 mM IPTG, 18°C, o.n. 50 µM $ZnCl_2$	1. IMAC: batch 2. TEV cleavage 3. IMAC: batch 4. Superdex 75	2H-I S4C
^{HisTEV}Pib1RING +50aa	pET30-His$_6$-TEV-Pib1RING+50aa (aa 175-286) (pHU3018)	BL21 CodonPlus (DE3) RIL 1 mM IPTG, 20°C, o.n. 50 µM $ZnCl_2$	1. IMAC: batch 2. Superdex S75	S1C S2A
^{HisTEV}Pib1RING +30aa	pET30-His$_6$-TEV-Pib1RING+30aa (aa 195-286) (pHU3017)	BL21 CodonPlus (DE3) RIL 1 mM IPTG, 20°C, o.n. 50 µM $ZnCl_2$	1. IMAC: batch 2. Superdex S75	S1C S2A
^{GST}Cue1^{His}	pGEX-6P-Cue1-His$_6$ (pHU2458)	BL21 pLysS 1 mM IPTG, 18°C, o.n.	(5) 1. GSH-Sepharose: batch 2. Superdex 200	2G
Hrd1(325-551)	pGEX-Hrd1(325-551) (pHU2459)	BL21 CodonPlus (DE3) RIL 1 mM IPTG, 18°C o.n. 50 µM $ZnCl_2$	(5) 1. GSH-Sepharose: batch 2. PreScission cleavage 3. GSH-Sepharose: batch 4. Superdex 200	3H S4A
^{GST}Rsp5	pGEX-6P-HA-Rsp5 (pHU3473)	Rosetta 2 0.1 mM IPTG, 16°C, o.n.	(6) GSH-Sepharose: batch	2F,I

RFFL(97-363) Iso1	pGEX-6P-1-RFFL (aa 97-363) Isoform 1 (pHU3016)	BL21 CodonPlus (DE3) RIL 1 mM IPTG, 18°C, o.n. 50 µM $ZnCl_2$	1. GSH-Sepharose: batch 2. PreScission cleavage 3. GSTrap HP 5 ml: 2 runs 4. Superdex 200	3E S4B,C
SpPib1(123-279)	pGEX-6P-1-SpPib1 (aa 123-279) (pHU3204)	BL21 pLysS 0.1 mM IPTG, 18°C, o.n. 50 µM $ZnCl_2$	1. GSH-Sepharose: batch 2. PreScission cleavage 3. GSH-Sepharose: batch 4. Superdex 75	3C S4C
Tul1(655-758)	pGEX-6P-1-Tul1 (aa 655-758) (pHU3741)	BL21 CodonPlus (DE3) RIL 1 mM IPTG, 18°C, o.n. 50 µM $ZnCl_2$	1. GSH-Sepharose: batch 2. PreScission cleavage 3. GSH-Sepharose: batch 4. Superdex 75	3F S4C
^{GST}Upa1(1131-1287)	pGEX-6P-1-Upa1 (aa 1131-1287) (pHU3025)	BL21 CodonPlus (DE3) RIL 1 mM IPTG, 20°C, o.n. 50 µM $ZnCl_2$	GSH-Sepharose: batch	3D S4C
^{GST}ZNRF2	pGEX-2TK-ZNRF2 (pHU3213)	BL21 CodonPlus (DE3) RIL 1 mM IPTG, 18°C, o.n. 50 µM $ZnCl_2$	GSH-Sepharose: batch	3G S4C

References:

(1) Hospenthal MK, Mevissen TET, Komander D (2015) Deubiquitinase-based analysis of ubiquitin chain architecture using Ubiquitin Chain Restriction (UbiCRest). *Nat Protoc* **10:** 349-361

(2) Carvalho AF, Pinto MP, Grou CP, Vitorino R, Domingues P, Yamao F, Sa-Miranda C, Azevedo JE (2012) High-yield expression in *Escherichia coli* and purification of mouse ubiquitin-activating enzyme E1. *Mol Biotechnol* **51:** 254-261

(3) Pickart CM, Raasi S (2005) Controlled synthesis of polyubiquitin chains. *Methods Enzymol* **399:** 21-36

(4) Branigan E, Plechanovova A, Jaffray EG, Naismith JH, Hay RT (2015) Structural basis for the RING-catalyzed synthesis of K63-linked ubiquitin chains. *Nat Struct Mol Biol* **22:** 597-602

(5) Bagola K, von Delbruck M, Dittmar G, Scheffner M, Ziv I, Glickman MH, Ciechanover A, Sommer T (2013) Ubiquitin binding by a CUE domain regulates ubiquitin chain formation by ERAD E3 ligases. *Mol Cell* **50:** 528-539

(6) Wang G, Yang J, Huibregtse JM (1999) Functional domains of the Rsp5 ubiquitin-protein ligase. *Mol Cell Biol* **19:** 342-352